PNAS RESEARCH ARTICLE | IMMUNOLOGY AND INFLAMMATION

SRC2 controls CD4$^+$ T cell activation via stimulating c-Myc-mediated upregulation of amino acid transporter *Slc7a5*

Wencan Zhang[a,1], Xu Cao[b,1], Xiancai Zhong[a], Hongmin Wu[a], Yun Shi[a], Mingye Feng[b], Yi-Chang Wang[c], David Ann[c], Yousang Gwack[d], Yate-Ching Yuan[e], Weirong Shang[f], and Zuoming Sun[a,2]

Edited by Douglas Green, St Jude Children's Research Hospital, Memphis, TN; received December 16, 2022; accepted March 16, 2023

T cell activation stimulates substantially increased protein synthesis activity to accumulate sufficient biomass for cell proliferation. The protein synthesis is fueled by the amino acids transported from the environment. Steroid nuclear receptor coactivator 2 (SRC2) is a member of a family of transcription coactivators. Here, we show that SRC2 recruited by c-Myc enhances CD4$^+$ T cell activation to stimulate immune responses via upregulation of amino acid transporter Slc7a5. Mice deficient of SRC2 in T cells (*SRC2$^{fl/fl}$/CD4^{Cre}*) are resistant to the induction of experimental autoimmune encephalomyelitis (EAE) and susceptible to *Citrobacter rodentium* (*C. rodentium*) infection. Adoptive transfer of naive CD4$^+$ T cells from *SRC2$^{fl/fl}$/CD4^{Cre}* mice fails to elicit EAE and colitis in *Rag1$^{-/-}$* recipients. Further, CD4$^+$ T cells from *SRC2$^{fl/fl}$/CD4^{Cre}* mice display defective T cell proliferation, cytokine production, and differentiation both in vitro and in vivo. Mechanically, SRC2 functions as a coactivator to work together with c-Myc to stimulate the expression of amino acid transporter Slc7a5 required for T cell activation. Slc7a5 fails to be up-regulated in CD4$^+$ T cells from *SRC2$^{fl/fl}$/CD4^{Cre}* mice, and forced expression of *Slc7a5* rescues proliferation, cytokine production, and the ability of *SRC2$^{fl/fl}$/CD4^{Cre}* CD4$^+$ T cells to induce EAE. Therefore, SRC2 is essential for CD4$^+$ T cell activation and, thus, a potential drug target for controlling CD4$^+$ T cell-mediated autoimmunity.

CD4$^+$ T cell | T cell activation | c-Myc | autoimmunity

T cell activation is the initial step in adaptive immune responses essential for clearing pathogen infection as well as for the induction of autoimmunity (1). T cell activation triggers the clonal expansion of a few antigen-specific naive T cells into a large pool of antigen-specific effector T cells required for the efficient clearance of pathogens that often propagate exponentially such as bacteria. Naive resting T cells are inactive and thus incapable of mediating immune responses. However, T cell receptor (TCR) engagement induces T cell proliferation and differentiation of naive T cells into effector T cells with cytokine production capabilities. Activated T cells must accumulate sufficient biomass before cell division, including protein and DNA, and reflected by greatly increased cell size. To meet the demands of substantially increased protein synthesis activity, activated T cells require the transport of amino acids, the building blocks of proteins, from the environment (2), and amino acid transporter expression increases up to 100-fold in activated T cells (3). Further, deletion of the genes encoding amino acid transporters, such as solute carrier family 7 member 5 (*Slc7a5*) and solute carrier family 1 member 5 (*Slc1a5*), markedly impairs T cell activation including proliferation and differentiation (3–6), demonstrating the critical function of amino acid transporters in T cell activation process.

Transcription factor c-Myc is responsible for stimulating the expression of the amino acid transporters during T cell activation, as deletion of c-Myc prevents the upregulation of amino acid transporters including *Slc7a5* (3). TCR stimulation rapidly induces c-Myc (7) whose expression is then increased at both transcriptional and translation levels (8–10). Interestingly, c-Myc-deficient T cells are unable to proliferate and differentiate in response to TCR stimulation; these T cells are also deficient in amino acid transporter Slc7a5, suggesting that Slc7a5 is an important downstream target of c-Myc during T cell activation. While it is known that c-Myc directly binds to the promoter region of *Slc7a5* to regulate its expression (11), it remains unknown about other factors that regulate *Slc7a5* expression.

Steroid receptor coactivator 2 (SRC2) belongs to a family of SRC coactivators (SRC) consisting of three members, SRC1 (or NCOA1), SRC2 (or NCOA2/TIF2/GRIP1), and SRC3 (or NCOA3/pCIP/ACTR/AIB1). SRCs do not directly bind to target DNA; they function as coactivators for steroid nuclear receptors and other transcription factors by interacting with them to regulate gene transcription (12). As such, SRCs orchestrate transcription programs critical for multiple cellular functions (12). However, the function of

Significance

Steroid receptor coactivator 2 belongs to a family of SRC coactivators, which orchestrate transcription programs critical for multiple cellular functions. However, the function of SRCs especially SRC2 in the immune system has long been ignored. Here, we show that SRC2 functions as a coactivator for c-Myc to stimulate the expression of amino acid transporter Slc7a5 required for T cell activation. Uncontrolled activation of T cells is responsible for various autoimmune diseases such as multiple sclerosis and immunological bowel disease and thus inhibiting the activity of SRC2 hypothetically can prevent such T cell-mediated autoimmunity. Our study not only reveals an important mechanism for SRC2-regulated T cell activation but also identifies SRC2 as a potential therapeutic target for T cell-mediated autoimmune diseases.

Author contributions: Z.S., W.Z., X.C. and Y.G. designed research; W.Z., X.C., X.Z., H.W., Y.S., Y-C.W., and W.S. performed research; D.A., Y-C.W., M.F., and Y-C.Y. contributed new reagents/analytic tools; Z.S., W.Z., X.C., X.Z., H.W., Y.S., Y-C.W., and W.S analyzed data; and W.Z., X.C., and Z.S. wrote the paper.

The authors declare no competing interest.

This article is a PNAS Direct Submission.

[1]W.Z. and X.C. contributed equally to this work.

[2]To whom correspondence may be addressed. Email: zsun@coh.org.

This article contains supporting information online at https://www.pnas.org/lookup/suppl/doi:10.1073/pnas.2221352120/-/DCSupplemental.

Published April 24, 2023.

SRCs in the immune system has long been ignored. Our previous study illustrated that SRC1 can reciprocally regulate the differentiation of inflammatory Th17 cells and Tregs by promoting Th17 while inhibiting Treg differentiation (13). Similar to SRC1, we and others showed that SRC3 promotes Th17 differentiation (14, 15). Therefore, SRC1 and SRC3 have nonredundant functions in stimulating Th17 differentiation. Although a recent report using germline *SRC3*$^{-/-}$ mice and SRC3 inhibitor hinted at a possible function of SRC3 in Treg differentiation (16), SRC3 was found dispensable for Treg differentiation using a T cell-specific SRC3 knockout mice (15). As for SRC2, we recently discovered its critical role in the differentiation of induced regulatory T cells (17). However, the function of SRC2 in conventional T cells remains unknown. In this study, we investigated the function of SRC2 in the regulation of CD4$^+$ T cell activation in vitro and in vivo.

Results

Mice Deficient of SRC2 in T Cells (*SRC2*$^{fl/fl}$/*CD4*^{Cre}) Display Defects in T Cell-Mediated Immune Responses. To determine the function of SRC2 in T cells, we crossed *SRC2*$^{fl/fl}$ mice to *CD4*^{Cre} mice (*SRC2*$^{fl/fl}$/*CD4*^{Cre}) to delete *SRC2* in T cell compartments, which was confirmed by the lack of SRC2 protein (*SI Appendix*, Fig. S1*A*) and mRNA (*SI Appendix*, Fig. S1*B*) in *SRC2*$^{fl/fl}$/*CD4*^{Cre} CD4$^+$ T cells. In contrast to mice (*SRC2*$^{fl/fl}$/*Foxp3*$^{YFP\text{-}Cre}$) with Treg-specific deletion of SRC2 that lost weight with aging due to autoimmunity (17), the body weight of *SRC2*$^{fl/fl}$/*CD4*^{Cre} mice was comparable to that of wild-type (WT) control *SRC2*$^{fl/fl}$ mice in both male and female at 8 to 20 wk of age (*SI Appendix*, Fig. S1*C*). Initial analysis of *SRC2*$^{fl/fl}$/*CD4*^{Cre} mice also did not find obvious defects in thymic cellularity (*SI Appendix*, Fig. S1*D*) and thymocyte development in terms of distribution of different developmental stages of thymocytes: CD4$^-$CD8$^-$ double-negative, CD4$^+$CD8$^+$ double-positive, and CD4$^+$ or CD8$^+$ single-positive cells (*SI Appendix*, Fig. S1*E*). Further, *SRC2*$^{fl/fl}$ and *SRC2*$^{fl/fl}$/*CD4*^{Cre} mice showed comparable spleen cellularity (*SI Appendix*, Fig. S1*F*), which was supported by a comparable percentage of CD19$^+$ B cells and CD3$^+$ T cells including CD4$^+$ and CD8$^+$ T cells in both spleens (*SI Appendix*, Fig. S1*G*) and iLNs (*SI Appendix*, Fig. S1*H*).

EAE was then induced by immunization with MOG$_{35–55}$ (18), and *SRC2*$^{fl/fl}$/*CD4*^{Cre} mice were resistant to EAE induction, indicated by delayed onset and much less severity (Fig. 1*A*) as well as greatly reduced incidence (Fig. 1*B*) of the disease when compared to *SRC2*$^{fl/fl}$ mice. A significant number of infiltrating CD45$^+$ lymphocytes (Fig. 1*C* and *SI Appendix*, Fig. S1*I* for gating strategy), including CD4$^+$ T cells (Fig. 1*D*) producing IL-17A and IFNγ

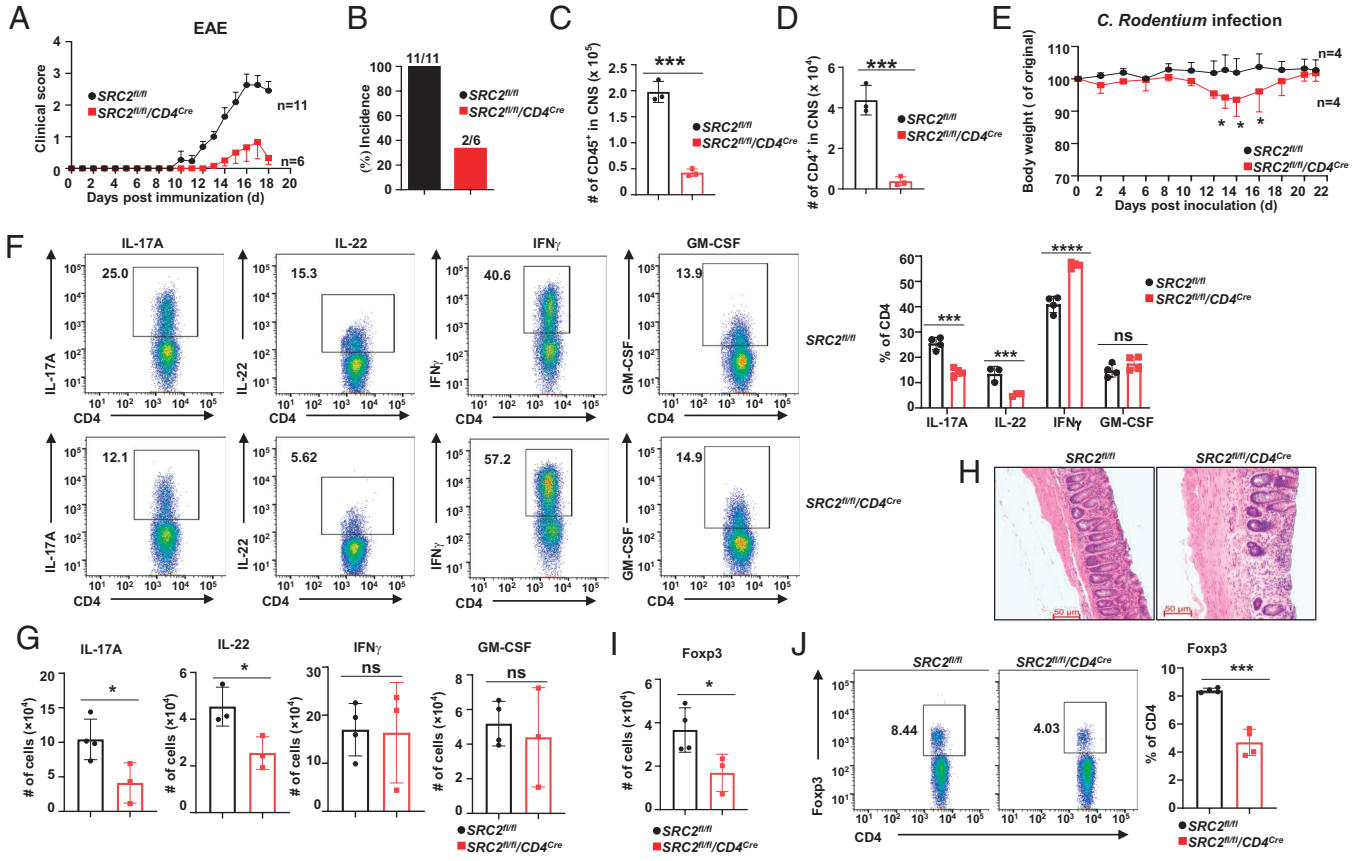

Fig. 1. Mice deficient of SRC2 in T cells (*SRC2*$^{fl/fl}$/*CD4*^{Cre}) display defects in T cell-mediated immune responses. (*A*) Mean clinical EAE scores of indicatedmice at different day post-EAE induction with MOG$_{35\text{-}55}$ (n ≥ 6 per genotype). (*B*) Incidence of paralysis of indicatedmice after EAE induction shown in *A* (n ≥ 6 per genotype). (*C* and *D*) Absolute number of CD45$^+$ (*C*) and CD4$^+$ (*D*) cells recovered from the CNS from indicated mice 18 d post EAE induction shown in *A* (n = 3 per genotype). (*E*) Body weight of indicated mice over time after *C. Rodentium* infection (n = 4 per genotype). (*F*) Representative flow cytometric analysis (*Left*) and the percentage (*Right*) of IL-17A$^+$, IL-22$^+$, IFNγ$^+$, and GM-CSF$^+$ cells among CD4$^+$ cells from the colon of indicated mice 3 wk after *C. Rodentium* infection shown in *E* (n = 4 per genotype). Numbers indicate the percentage of the cells in the gated area (throughout). (*G*) Absolute number of IL-17A$^+$, IL-22$^+$, IFNγ$^+$, and GM-CSF$^+$ cells in the colon from indicated mice 3 wk after *C. Rodentium* infection shown in *F* (n ≥ 3 per genotype). (*H*) Hematoxylin and Eosin (H&E)-stained colon section of indicated mice 3 wk after *C. Rodentium* infection shown in *E*. (*I*) Absolute number of CD4$^+$Foxp3$^+$ cells in the colon from indicated mice 3 wk after *C. Rodentium* infection shown in *E* (n ≥ 3 per genotype). (*J*) Representative flow cytometric analysis (*Left*) and the percentage (*Right*) of Foxp3$^+$ cells among CD4$^+$ T cells in the colon from indicated mice 3 wk after *C. Rodentium* infection shown in *E* (n = 3 per genotype). Data are from three experiments (*A–G* and *I*; *F* and *J*, *Right* panels; data in *C–E*, *G*, and *I*; *F* and *J*, *Right* panels are presented as mean ± SD; data in *A* are presented as mean ± SEM) or are from one representative of three independent experiments (*H*; *F* and *J*, *Left* panels). *P < 0.01; ***P < 0.001; ****P < 0.0005; ns, not significant (two-tailed Students' t test).

(*SI Appendix*, Fig. S1 *J* and *K*), were recovered from the central nervous system (CNS) of *SRC2*$^{fl/fl}$ mice. However, there were very few CD45$^+$ infiltrating lymphocytes (Fig. 1*C*), including CD4$^+$ T cells (Fig. 1*D*) recovered from CNS of *SRC2*$^{fl/fl}$/*CD4*^{Cre} mice, indicating a lack of inflammation that causes EAE. SRC2 is thus required to generate T cell-mediated immune responses involved in the induction of EAE.

While EAE results from T cell activation by self-antigen in CNS, we next determined the function of SRC2 in T cell responses to the pathogen *Citrobacter rodentium* (*C. rodentium*). Clearance of *C. rodentium* infection depends on T cells, as mice lacking T cells are highly susceptible to infection by this strain of bacteria (19, 20). *C. rodentium* infection caused more weight loss in *SRC2*$^{fl/fl}$/*CD4*^{Cre} mice compared to *SRC2*$^{fl/fl}$ mice (Fig. 1*E*), suggesting ineffective immune responses against infection. *C. rodentium* induces inflammation, indicated by lymphocyte infiltration, including IL-17- and IL-22-producing CD4$^+$ T cells, which play an important role in clearing *C. rodentium* infection (21, 22). Indeed, a greatly reduced percentage (Fig. 1*F* and *SI Appendix*, Fig. S1*L* for gating strategy) and number (Fig. 1*G*) of IL-17A$^+$ and IL-22$^+$ but not IFNγ$^+$ and GM-CSF$^+$ CD4$^+$ T cells were recovered from the colon of infected *SRC2*$^{fl/fl}$/*CD4*^{Cre} mice compared to that of *SRC2*$^{fl/fl}$ mice, supporting impaired immune responses against *C. rodentium* infection in *SRC2*$^{fl/fl}$/*CD4*^{Cre} mice. In addition, uncontrolled *C. rodentium* infection also caused more tissue damage in the colon including hyperplasia and damaged crypts in *SRC2*$^{fl/fl}$/*CD4*^{Cre} mice (Fig. 1*H*). Consistent with our previously reported requirement of SRC2 for the generation of induced Treg (17), there were reduced number (Fig. 1*I*) and percentage (Fig. 1*J* and *SI Appendix*, Fig. S1*L* for gating strategy) of Tregs in the colon but not spleen and lymph node (*SI Appendix*, Fig. S1*M*) of *SRC2*$^{fl/fl}$/*CD4*^{Cre} mice. However, reduced Tregs cannot explain impaired T cell-dependent immune responses against *C. rodentium* infection. Our results thus support the critical role of SRC2 in T cell-mediated immune responses.

CD4$^+$ T Cells from SRC2$^{fl/fl}$/CD4^{Cre} Mice Are Defective in the Induction of EAE and Colitis. As *SRC2* is deleted in the entire T cell compartments of *SRC2*$^{fl/fl}$/*CD4*^{Cre} mice, we next determined the function of SRC2 specifically in CD4$^+$ T cells. For this purpose, CD4$^+$ T cells were purified from *SRC2*$^{fl/fl}$ or *SRC2*$^{fl/fl}$/*CD4*^{Cre} mice and adoptively transferred to *Rag1* mice that were then induced to develop EAE (*SI Appendix*, Fig. S2*A*). In contrast to *SRC2*$^{fl/fl}$ CD4$^+$ T cells, CD4$^+$ T from *SRC2*$^{fl/fl}$/*CD4*^{Cre} mice failed to induce any sign (Fig. 2*A*) and incidence (Fig. 2*B*) of EAE in *Rag1* recipients. Consistently, there were significantly fewer CD45$^+$ infiltrating lymphocytes (Fig. 2*C*), including CD4$^+$ T cells (Fig. 2*D*) recovered from CNS of *Rag1* mice reconstituted with *SRC2*$^{fl/fl}$/*CD4*^{Cre} CD4$^+$ T cells than from *Rag1* mice reconstituted with *SRC2*$^{fl/fl}$ CD4$^+$ T cells. In contrast, there were a higher number of CD4$^+$ T cells in the spleens (*SI Appendix*, Fig. S2*B*) of the *Rag1* mice reconstituted with *SRC2*$^{fl/fl}$/*CD4*^{Cre} CD4$^+$ T cells compared to mice reconstituted with *SRC2*$^{fl/fl}$ CD4$^+$ T cells. This is presumably due to the mobilization of substantially more *SRC2*$^{fl/fl}$ than *SRC2*$^{fl/fl}$/*CD4*^{Cre} CD4$^+$ T cells from the spleen to CNS for induction of EAE. Histological analysis revealed more infiltrating lymphocytes and tissue damage (demyelination) in the brain (Fig. 2*E*) and spinal cord (Fig. 2*F*) of *Rag1* mice with *SRC2*$^{fl/fl}$ CD4$^+$ T cells compared to *Rag1* mice with *SRC2*$^{fl/fl}$/*CD4*^{Cre} CD4$^+$ T cells. SRC2 is thus required for the development of CD4$^+$ T cell-mediated EAE.

Next, we determined the function of SRC2 in colitis induced by the adoptive transfer of naive CD4$^+$ T cells (23). Adoptive transfer of naive *SRC2*$^{fl/fl}$ but not *SRC2*$^{fl/fl}$/*CD4*^{Cre} CD4$^+$ T cells induced severe colitis in *Rag1* recipients, indicated by weight loss (Fig. 2*G*), shortened colon (Fig. 2 *H*, *Left* and *I*), and colon tissue damage such as hyperplasia (Fig. 2*J*). Smaller spleens (Fig. 2 *H*, *Right*) together with significantly fewer total number of splenocytes (*SI Appendix*, Fig. S2*C*), including CD4$^+$ T cells (*SI Appendix*, Fig. S2*D*) that produce IFNγ and IL-17A (*SI Appendix*, Fig. S2 *E* and *F* for gating strategy), were found in *Rag1* mice with *SRC2*$^{fl/fl}$/*CD4*^{Cre} CD4$^+$ T cells than mice with *SRC2*$^{fl/fl}$ CD4$^+$ T cells, indicating diminished inflammation in the absence of SRC2. Indeed, fewer inflammatory CD45$^+$ lymphocytes (Fig. 2 *K*, *Left*), CD4$^+$ T cells (Fig. 2 *K*, *Right*) that produce IFNγ (Fig. 2 *L*, *Left* and *SI Appendix*, Fig. S2*G* for gating strategy) and IL-17A (Fig. 2 *L*, *Right*) were recovered from the colon of *Rag1* mice with *SRC2*$^{fl/fl}$/*CD4*^{Cre} CD4$^+$ T cells than from mice with *SRC2*$^{fl/fl}$ CD4$^+$ T cells. Moreover, although naive CD4$^+$ T cells from both *SRC2*$^{fl/fl}$ and *SRC2*$^{fl/fl}$/*CD4*^{Cre} mice had equally low levels of surface T cell activation marker CD44 (*SI Appendix*, Fig. S2*H*), CD4$^+$ T cells recovered from the colon (Fig. 2*M*) and mesenteric lymph nodes (mLN) (Fig. 2*N*) of *Rag1* mice with *SRC2*$^{fl/fl}$/*CD4*^{Cre} CD4$^+$ T cells expressed lower levels of CD44 than those recovered from mice with *SRC2*$^{fl/fl}$ CD4$^+$ T cells, indicating the defective T cell activation in the absence of SRC2. SRC2 is thus essential for CD4$^+$ T cell function, as deletion of SRC2 almost abrogated CD4$^+$ T cell-mediated immune responses involved in both EAE and colitis.

CD4$^+$ T Cells from SRC2$^{fl/fl}$/CD4^{Cre} Mice Are Defective in T Cell Activation. Since our results above indicated that defective T cell activation is responsible for the lack of immune responses by CD4$^+$ T cells from *SRC2*$^{fl/fl}$/*CD4*^{Cre} mice, we further examined the role of SRC2 in T cell activation. Upon activation by anti-CD3/CD28 antibodies, *SRC2*$^{fl/fl}$/*CD4*^{Cre} CD4$^+$ T cells displayed defects in proliferation (Fig. 3*A*) and upregulation of activation markers CD25 (Fig. 3*B*) and CD69 (*SI Appendix*, Fig. S3*A*). However, there was no obvious difference in the survival between CD4$^+$ T cells from *SRC2*$^{fl/fl}$ and *SRC2*$^{fl/fl}$/*CD4*^{Cre} mice (*SI Appendix*, Fig. S3 *B* and *C*). Activation with PMA and ionomycin led to similar defects in proliferation (Fig. 3*C*) and upregulation of activation marker CD69 (*SI Appendix*, Fig. S3*D*) in *SRC2*$^{fl/fl}$/*CD4*^{Cre} CD4$^+$ T cells. We further used *OT-II* transgenic mice that express TCR recognizing Ova to monitor CD4$^+$ T cell activation by antigen-presenting cells (APCs). CD4$^+$ cells from *OT-II*/*SRC2*$^{fl/fl}$/*CD4*^{Cre} showed more dramatic defects than above activated by CD3/CD28 cross-linking in the upregulation of activation marker CD25 (Fig. 3*D*). This result indicates that overwhelming stimulation by CD3/28 cross-link could overcome the defective activation of *SRC2*$^{fl/fl}$/*CD4*^{Cre} T cells. We next examined T cell differentiation. Naive CD4$^+$ T cells from *SRC2*$^{fl/fl}$ and *SRC2*$^{fl/fl}$/*CD4*^{Cre} mice did not produce IFNγ or IL-17A (*SI Appendix*, Fig. S3*E*). However, *SRC2*$^{fl/fl}$/*CD4*^{Cre} CD4$^+$ T cells showed a defective Th17 differentiation when activated under two different Th17 polarization conditions, IL-6 + TGFβ + IL-23 (Fig. 3*E*) or IL-6 + TGFβ (*SI Appendix*, Fig. S3*F*) for 45 h (Fig. 3*E* and *SI Appendix*, Fig. S3 *F*, *Top* panels) or 72 h (Fig. 3*E* and *SI Appendix*, Fig. S3 *F*, *Bottom*). *SRC2*$^{fl/fl}$/*CD4*^{Cre} CD4$^+$ T cells showed greatly decreased ability to differentiate into IL-17A- but not IFNγ-producing cells, which was confirmed by qPCR (*SI Appendix*, Fig. S3*G*). Defective Th17 differentiation was also observed under another Th17 polarization conditions, IL-6 + IL-1β + IL-23 (*SI Appendix*, Fig. S3*H*); however, there was an increased IFNγ production by *SRC2*$^{fl/fl}$/*CD4*^{Cre} CD4$^+$ T cells. Further analysis under Th1 polarization conditions demonstrated that *SRC2*$^{fl/fl}$/*CD4*^{Cre} and *OT-II*/*SRC2*$^{fl/fl}$/*CD4*^{Cre} CD4$^+$ T cells both showed increased differentiation into IFNγ-producing Th1 cells (Fig. 3 *F* and *G*). Our in vitro analysis thus supports the essential function of SRC2 in CD4$^+$ T cell activation-induced proliferation and Th17 differentiation.

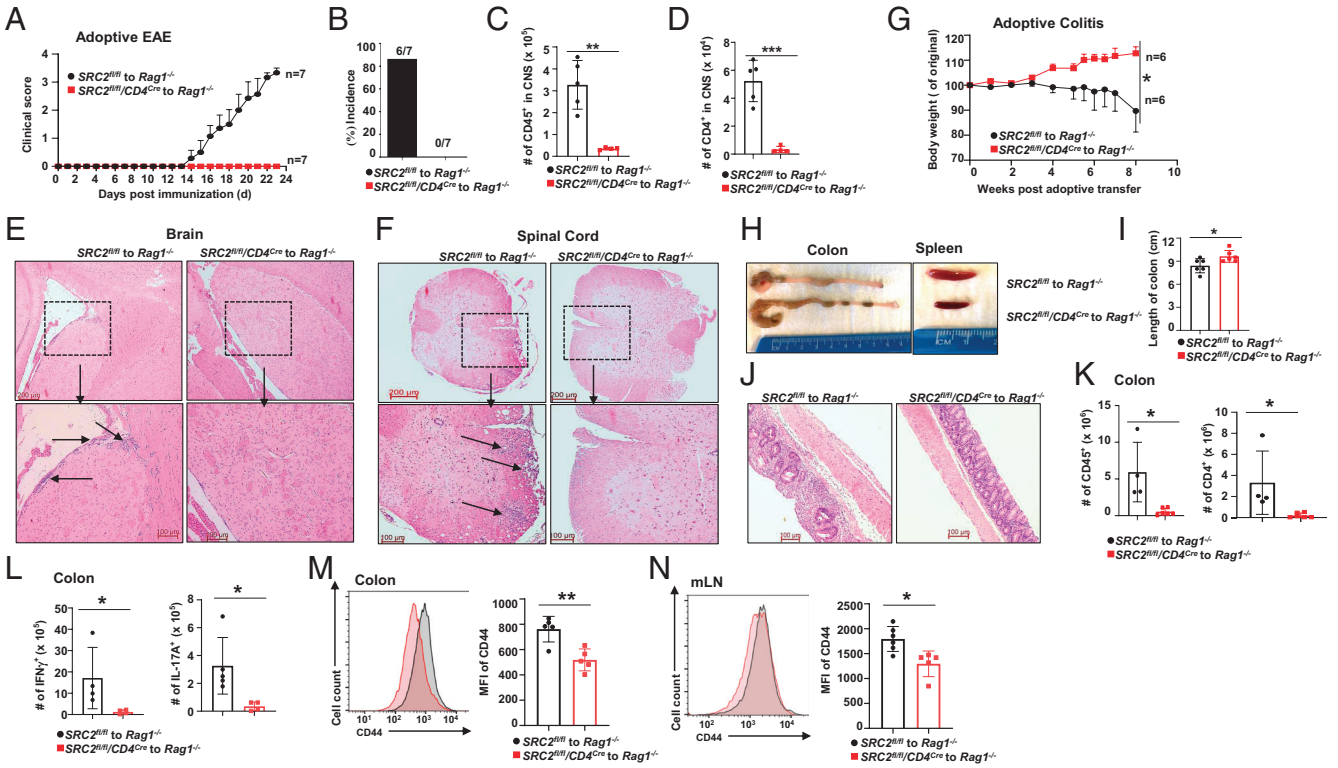

Fig. 2. Naive CD4$^+$ T cells from *SRC2$^{fl/fl}$/CD4^{Cre}* mice are defective in the induction of EAE and colitis. (*A*) Mean clinical EAE scores of *Rag1$^{-/-}$* mice adoptively transferred with CD4$^+$ cells from indicated mice at different days post-EAE induction with MOG_{35-55} (n = 7 per genotype). (*B*) Incidence of paralysis of indicated *Rag1$^{-/-}$* recipients after EAE induction with MOG_{35-55} shown in *A* (n = 7 per genotype). (*C* and *D*) Absolute number of CD45$^+$ (*C*) and CD4$^+$ (*D*) cells in the CNS from indicated *Rag1$^{-/-}$* recipients shown in A post-EAE induction (n ≥ 4 per genotype). (*E* and *F*) Section of H&E-stained brain (*E*) and spinal cord (*F*) from *Rag1$^{-/-}$* recipients post-EAE induction shown in *A*. (*G*) Body weight of *Rag1$^{-/-}$* recipients over time post-adoptive transfer of indicated naive CD4$^+$ T cells (n = 6 per genotype). (*H*) Images of colons (*Left*) and spleens (*Right*) from *Rag1* recipients 8 wk after adoptive transfer of indicated naive CD4$^+$ T cells shown in *G*. (*I* and *J*). Colon length (*I*, n = 6 per genotype) and H&E-stained colon section (*J*) from *Rag1* recipients 8 wk after adoptive transfer of indicated naive CD4$^+$ T cells shown in *G*. (*K*) Absolute number of CD45$^+$ (*Left*) and CD4$^+$ (*Right*) cells in the colon from *Rag1* recipients 8 wk after adoptive transfer of indicated naive CD4$^+$ T cells shown in *G* (n ≥ 4 per genotype). (*L*) Absolute number of CD4$^+$IFNγ$^+$ (*Left*) and CD4$^+$IL-17A$^+$ (*Right*) cells in the colon from *Rag1* recipients 8 wk after adoptive transfer of indicated naive CD4$^+$ T cells shown in *G* (n ≥ 4 per genotype). (*M* and *N*) Representative flow cytometric analysis (*Left*) and the MFI (*Right*) of CD44 among CD4$^+$ cells in the colon (*M*) and mesenteric lymph nodes (mLN) (*N*) from *Rag1$^{-/-}$* recipients 8 wk after adoptive transfer of indicated naive CD4$^+$ T cells shown in *G* (n ≥ 5 per genotype). Data are from three experiments (*A–D*, *G*, *I*, *K*, and *L*; *M* and *N*, *Right* panel; data in *C*, *D*, *I*, *K*, and *L*; *M* and *N*, *Right* panel are presented as mean ± SD; data in *A* and *G* are presented as mean ± SEM) or are from one representative of three independent experiments (*E*, *F*, *H*, and *J*; *M* and *N*, *Left* panels). *P < 0.01; **P < 0.005, ***P < 0.001 (two-tailed Students' t test).

We next examined T cell activation in vivo. A low number of naive CD4$^+$ T cells purified from *SRC2$^{fl/fl}$* or *SRC2$^{fl/fl}$/CD4^{Cre}* mice were adoptively transferred to *Rag1$^{-/-}$* mice to observe lymphopenia-induced proliferation (*SI Appendix*, Fig. S4*A*). Three weeks after adoptive transfer, *Rag1* mice with *SRC2$^{fl/fl}$/CD4^{Cre}* CD4$^+$ T cells had obviously much smaller spleen and lymph nodes than *Rag1* mice with *SRC2$^{fl/fl}$* CD4$^+$ T cells (Fig. 4*A*). Indeed, there were a considerably less total number of cells (*SI Appendix*, Fig. S4*B*), including a greatly reduced number of CD4$^+$ T cells in the spleens and lymph nodes (Fig. 4*B*) in *Rag1* mice with *SRC2$^{fl/fl}$/CD4^{Cre}* CD4$^+$ T cells, supporting defects in T cell proliferation in the absence of SRC2. Further, the percentage (Fig. 4*C*) and number (Fig. 4*D*) of IL-17A-producing CD4$^+$ T cells in the spleens of the *Rag1* mice with *SRC2$^{fl/fl}$/CD4^{Cre}* CD4$^+$ T cells were also much lower compared to that of *Rag1* mice with *SRC2$^{fl/fl}$* CD4$^+$ T cells, confirming the role of SRC2 in generating Th17 cells.

To monitor antigen-specific T cell activation in vivo, we used *OT-II* transgenic mice (*OT-II/SRC2$^{fl/fl}$* and *OT-II/SRC2$^{fl/fl}$/CD4^{Cre}*) (*SI Appendix*, Fig. S4*C*). As expected, naive CD4$^+$ T cells from *OT-II/SRC2$^{fl/fl}$* and *OT-II/SRC2$^{fl/fl}$/CD4^{Cre}* mice expressed comparable low levels of activation markers CD69 (*SI Appendix*, Fig. S4*D*) and CD25 (*SI Appendix*, Fig. S4*E*) before adoptive transfer. CD4$^+$ T cells were then labeled with dye for monitoring proliferation CellTrace Violet (CTV, *SI Appendix*, Fig. S4*F*) and adoptively transferred to *Rag1* mice. Upon Ova immunization, CD4$^+$ T cells from *OT-II/SRC2$^{fl/fl}$/CD4^{Cre}* mice displayed very severe defective proliferation (Fig. 4*E*) and upregulation of activation markers CD69 and CD25 (Fig. 4 *F* and *G*). While we could not detect IL-17A$^+$ cells, there were consistently higher percentage of IFNγ-producing (Fig. 4*H*) CD4$^+$ T cells from *OT-II/SRC2$^{fl/fl}$/CD4^{Cre}* mice compared to *OT-II* WT mice. In addition, when naive CD4$^+$ T cells from *OT-II/SRC2$^{fl/fl}$* and *OT-II/SRC2$^{fl/fl}$/CD4^{Cre}* mice were transferred to WT mice, consistent with previous findings, *OT-II/SRC2$^{fl/fl}$/CD4^{Cre}* CD4$^+$ cells also showed severe defective proliferation (*SI Appendix*, Fig. S4*G*) and upregulation of activation markers CD69 (*SI Appendix*, Fig. S4*H*). SRC2 is thus required for CD4$^+$T cell activation-induced proliferation and Th17 differentiation in vivo.

Given the dramatic defects in vivo, we noticed that the defects in activation and proliferation in vitro are relatively mild between *SRC2$^{fl/fl}$* and *SRC2$^{fl/fl}$/CD4^{Cre}* CD4$^+$ T cells. One explanation would be that the nutrients are more enriched and ready to be used in culture medium than that in vivo, which may overcome the defects in activation of *SRC2$^{fl/fl}$/CD4^{Cre}* CD4$^+$ T cells. We thus tested the proliferation and activation of CD4$^+$ cells in a nutrition-restricted medium and found more dramatic defects of proliferation (*SI Appendix*, Fig. S4*I*) and upregulation of activation marker CD25 (*SI Appendix*, Fig. S4*J*) in *SRC2$^{fl/fl}$/CD4^{Cre}* CD4$^+$ T cells compared to that stimulated in the regular nutrition-enriched medium (Fig. 3 *A–C*). This result suggests

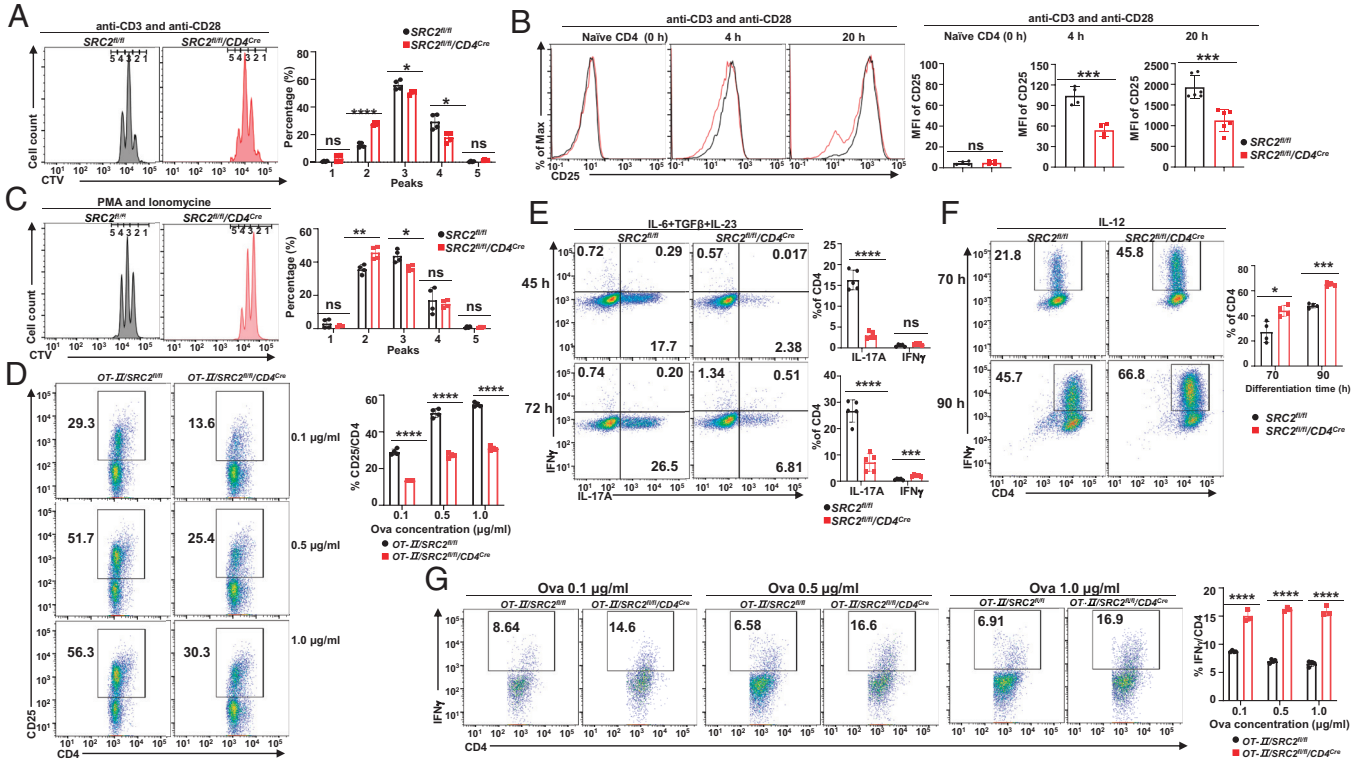

Fig. 3. CD4$^+$ T cells from *SRC2$^{fl/fl}$/CD4^{Cre}* mice are defective in T cell activation in vitro. (*A*) Representative flow cytometric analysis (*Left*) and percentage (*Right*) of the indicated proliferating CD4$^+$ T cells labeled with CellTrace Violet (CTV), stimulated with anti-CD3/28 antibodies for 42 h (n = 4 per genotype). (*B*) Representative flow cytometric analysis (*Left*) and MFI (*Right*) of CD25 on indicated CD4$^+$ T cells stimulated with anti-CD3/28 antibodies for the indicated times (0 h, 4 h and 20 h) (n ≥ 4 per genotype). (*C*) Representative flow cytometric analysis (*Left*) and percentage (*Right*) of the indicated proliferating CD4$^+$ T cells labeled with CTV and stimulated with PMA+ Ionomycin for 42 h (n = 4 per genotype). (*D*) Representative flow cytometric analysis (*Left*) and the percentage of CD25 (*Right*) on CD4$^+$ T cells from indicated mice after stimulation with different concentrations of Ova-loaded APCs for 24 h (n = 4 per genotype). (*E*) Representative flow cytometric analysis (*Left*) and the percentage (*Right*) of IL-17A$^+$ and IFNγ$^+$ cells among indicated CD4$^+$ T cells differentiated under Th17 polarization conditions (IL-6+ TGFβ+IL-23) for 45 h and 72 h (n = 4 per genotype). (*F*) Representative flow cytometric analysis (*Left*) and the percentage (*Right*) of IFNγ$^+$ cells among indicated CD4$^+$ T cells differentiated under Th1 polarization conditions for 70 h and 90 h (n = 4 per genotype). (*G*) Representative flow cytometric analysis (*Left*) and the percentage of IFNγ (*Right*) in CD4$^+$ T cells from indicated mice after stimulation with different concentrations of Ova-loaded APCs for 72 h (n = 4 per genotype). Boxed area: cell population of interest. Data are from three experiments (*A–G*, *Right* panels; presented as mean ± SD) or are from one representative of three independent experiments (*A–G*, *Left* panels). *P < 0.01; **P < 0.005; ***P < 0.001; ****P < 0.0005; ns, not significant (two-tailed Students' t test).

that nutrition availability limits the activation of *SRC2$^{fl/fl}$/CD4^{Cre}* CD4$^+$ T cells.

CD4$^+$ T Cells from SRC2$^{fl/fl}$/CD4^{Cre} Mice Are Defective in c-Myc-Dependent Pathways. Since SRC2 is a transcription coactivator that regulates cellular function via controlling gene expression, we performed RNA-seq analysis to determine SRC2-regulated genes after the adoptive transfer of *SRC2$^{fl/fl}$* and *SRC2$^{fl/fl}$/CD4^{Cre}* CD4$^+$ T cells (*SI Appendix*, Fig. S5*A*). The computational principal component analysis revealed that eight RNA-seq samples were divided into *SRC2$^{fl/fl}$* or *SRC2$^{fl/fl}$/CD4^{Cre}* group (*SI Appendix*, Fig. S5*B*), indicating reproducible gene expression patterns within each group and thus the high quality of RNA-seq results. We identified 2743 differentially expressed genes (DEGs), with 1408 up-regulated and 1335 down-regulated genes, between *SRC2$^{fl/fl}$* and *SRC2$^{fl/fl}$/CD4^{Cre}* CD4$^+$ cells (Fig. 5*A*). *Ncoa2,* which encodes SRC2, was among the most down-regulated genes (Fig. 5 *A*, *Left* and *SI Appendix*, Fig. S5*C*), confirming deletion of this gene. KEGG pathway analysis of DEGs identified many dysregulated pathways in *SRC2$^{fl/fl}$/CD4^{Cre}* cells; the most enriched pathways include DNA replication, cell cycle, and amino acid metabolism critical for cell proliferation (Fig. 5*B*). Cell proliferation required ATP to provide energy for cellular activities including DNA replication and protein synthesis (24). Indeed, *SRC2$^{fl/fl}$/CD4^{Cre}* CD4$^+$ cells generated much less ATP compared to *SRC2$^{fl/fl}$* cells (Fig. 5*C*), consistent with the observed defective proliferation in the absence of SRC2, implying defective metabolic pathways. We next compared the expression of the important genes known to regulate metabolisms required for T cell activation and proliferation (25) (*SI Appendix*, Fig. S5*D*). We found that *Hif1a*, *Batf*, *Myc,* and *Irf4* were down-regulated in *SRC2$^{fl/fl}$/CD4^{Cre}* CD4$^+$ cells from RNA-seq (Fig. 5*D*), and qPCR analysis confirmed the downregulation of *Hif1a* and *Baft* (Fig. 5*E*). The top down-regulated gene was *Hif1a*, which is known to promote T cell activation and Th17 differentiation (26, 27). Indeed, *SRC2$^{fl/fl}$/CD4^{Cre}* CD4$^+$ cells also had impaired Th17 differentiation in addition to defective T cell activation (Figs. 3 and 4). Down-regulated *Hif1a* at mRNA (*SI Appendix*, Fig. S5*E*) and protein levels (*SI Appendix*, Fig. S5*F*) were also confirmed in in vitro activated *SRC2$^{fl/fl}$/CD4^{Cre}* CD4$^+$ cells. However, forced expression of *Hif1a* did not rescue defective proliferation (*SI Appendix*, Fig. S5*G*) or Th17 differentiation (*SI Appendix*, Fig. S5*H*) of *SRC2$^{fl/fl}$/CD4^{Cre}* CD4$^+$ cells, suggesting other defects in the absence of SRC2.

DEGs were then subjected to upstream regulator analysis by Ingenuity Pathway Analysis (IPA) to search for dysregulated upstream regulators and c-Myc was identified as the top transcription factor responsible for the altered gene expression pattern in *SRC2$^{fl/fl}$/CD4^{Cre}* CD4$^+$ cells (Fig. 5*F*). Indeed, down-regulated c-Myc activity was directly linked to the altered expression of more than 150 known c-Myc target genes in *SRC2$^{fl/fl}$/CD4^{Cre}* CD4$^+$ cells from RNA-seq results (*SI Appendix*, Fig. S5*I*). Deletion of c-Myc prevents T cell activation (5, 28, 29), similar to the deletion of

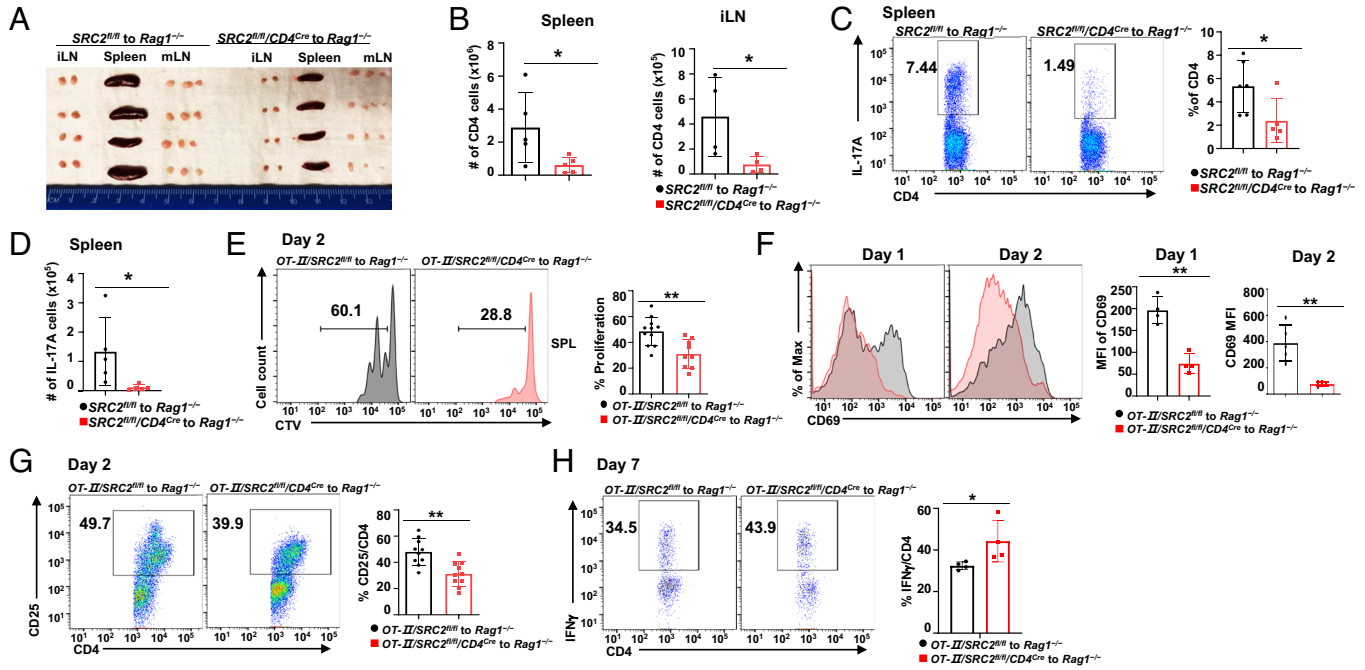

Fig. 4. CD4$^+$ T cells from *SRC2$^{fl/fl}$/CD4^{Cre}* mice are defective in T cell activation in vivo. (*A*) Representative image of iLNs, spleens, and mesenteric lymph nodes (mLNs) from *Rag1$^{-/-}$* recipients 3 wk post adoptively transfer of 0.4 × 10^6 naive CD4$^+$ cells from indicated mice. (*B*) Absolute number of CD4$^+$ T cells in the spleens (*Left*) and iLNs (*Right*) from *Rag1$^{-/-}$* recipients 3 wk post adoptively transfer of indicated naive CD4$^+$ cells shown in *A* (n ≥ 4 per genotype). (*C*) Representative flow cytometric analysis (*Left*) and the percentage (*Right*) of IL-17A$^+$ cells among CD4$^+$ T cells from the spleens of *Rag1$^{-/-}$* recipients 3 wk post adoptive transfer of indicated naive CD4$^+$ cells shown in *A* (n = 5 per genotype). (*D*) Absolute number of IL-17A$^+$ cells in the spleens from *Rag1$^{-/-}$* recipients 3 wk post adoptively transfer of indicated naive CD4$^+$ cells shown in *C* (n = 5 per genotype). (*E*) Representative flow cytometric analysis (*Left*) and percentage (*Right*) of the indicated proliferating CD4$^+$ T cells labeled with CTV 2 d after being adoptively transferred to *Rag1$^{-/-}$* recipients and stimulated by Ova immunization (n = 10 per genotype). (*F*) Representative flow cytometric analysis (*Left*) and the MFI (*Right*) of CD69 among indicated CD4$^+$ T cells in the spleens of *Rag1$^{-/-}$* recipients, 1 d (*Top* two panels) and 2 d (*Bottom* two panels) after Ova immunization shown in *E* (n ≥ 4 per genotype). (*G*) Representative flow cytometric analysis (*Left*) and the percentage of CD25$^+$ cells (*Right*) among indicated CD4$^+$ T cells in the spleen of *Rag1$^{-/-}$* recipients 2 d after Ova immunization shown in *E* (n = 10 per genotype). (*H*) Representative flow cytometric analysis (*Left*) and the percentage of IFNγ$^+$ cells among CD4$^+$ T cells (*Right*) in the spleen of *Rag1$^{-/-}$* recipients 7 d after Ova immunization shown in *L* (n = 4 per genotype). Boxed area: cell population of interest. Data are from three experiments (*B* and *D*; *C* and *E–H*, *Right* panels; presented as mean ± SD) or are from one representative of three independent experiments (*A*; *C* and *E–H*, *Left* panels). *P < 0.01; **P < 0.005, (two-tailed Students' t test).

SRC2. c-Myc is known to regulate multiple metabolic genes, including glycolysis and amino acid transportation essential for T cell activation (*SI Appendix*, Fig. S5*J*). Indeed, critical genes involved in these c-Myc-regulated metabolic pathways were down-regulated in *SRC2$^{fl/fl}$/CD4^{Cre}* CD4$^+$ cells (Fig. 5*G* and *SI Appendix*, Fig. S5*K*), and the mRNA levels of the most down-regulated genes were confirmed by individual qPCR (Fig. 5*H*). Computational analysis of RNA-seq data thus indicates defective c-Myc-dependent pathways in the absence of SRC2.

c-Myc Recruits SRC2 to Stimulate Transcription. We next determined whether the computational analysis predicted downregulation of c-Myc activity is responsible for defective activation of *SRC2$^{fl/fl}$/CD4^{Cre}* CD4$^+$ cells. Forced expression of c-Myc only slightly reversed defective proliferation (Fig. 6*A*) of *SRC2$^{fl/fl}$/CD4^{Cre}* CD4$^+$ cells but showed no effects on Th17 differentiation (Fig. 6*B*) of either *SRC2$^{fl/fl}$* or *SRC2$^{fl/fl}$/CD4^{Cre}* CD4$^+$ cells. We next monitored c-Myc protein levels, which were very low in unstimulated naive *SRC2$^{fl/fl}$* and *SRC2$^{fl/fl}$/CD4^{Cre}* CD4$^+$ cells (Fig. 6 *C*, *Top Left* and *SI Appendix*, Fig. S6*A* for the full image of the gel). Consistent with previous reports (5, 30), c-Myc is greatly up-regulated in *SRC2$^{fl/fl}$* CD4$^+$ T cells in response to TCR stimulation. Activated *SRC2$^{fl/fl}$/CD4^{Cre}* CD4$^+$ cells also up-regulated c-Myc to the levels that were only slightly lower than the WT cells (Fig. 6 *C* and *D*, *Top*), indicating that c-Myc is not likely regulated at the protein level. Since SRC2 is a transcriptional coactivator, we determined whether SRC2 can stimulate c-Myc transcriptional activity. Indeed, c-Myc together with SRC2 but not alone maximally stimulated the c-Myc luciferase reporter (Fig. 6*E*). In addition, CRISPR/Cas9-mediated knockdown of SRC2 (sgSRC2) but not nontargeting control (sgNTC) significantly impaired c-Myc-dependent activation of the reporter (Fig. 6*F*), suggesting that SRC2 functions as a coactivator to stimulate c-Myc activity. Further, c-Myc and SRC2 form protein complexes and could be defected in the same complexes after, but not before, stimulation of CD4$^+$ T cells by anti-CD3/CD28 antibodies (Fig. 6 *C* and *D*, *Bottom* and *SI Appendix*, Fig. S6*B* for full image of the gel) or Th17 differentiation conditions (*SI Appendix*, Fig. S6 *C* and *B*, *Right* panel for the full image of the gel). These results thus suggest that c-Myc recruits SRC2 to stimulate transcription. It could explain why the forced expression of c-Myc could not rescue the defective activation of *SRC2$^{fl/fl}$/CD4^{Cre}* CD4$^+$ cells, as c-Myc is unlikely able to fully activate some target genes without coactivator SRC2.

SRC2 Regulates CD4$^+$ T Cell Activation by Controlling c-Myc-Dependent Expression of Amino Acid Transporter Slc7a5. c-Myc regulates many pathways including well-known glycolysis and amino acid transportation (28). However, *SRC2$^{fl/fl}$/CD4^{Cre}* CD4$^+$ cells displayed rather increased than decreased glycolysis (*SI Appendix*, Fig. S7 *A* and *B*) and no obvious changes in oxidative phosphorylation (*SI Appendix*, Fig. S7 *C* and *D*) in response to TCR stimulation, not supporting the positive role of SRC2 in these two processes. In addition, c-Myc is responsible for the upregulation of multiple amino acid transporters that import basic building blocks to fuel the high levels of protein synthesis in proliferating T cells (2). Indeed, several amino acids metabolism pathways were found altered from RNA-seq results (Fig. 5*B*). Pharmacological inhibition or deletion of the genes encoding amino acid transporters severely

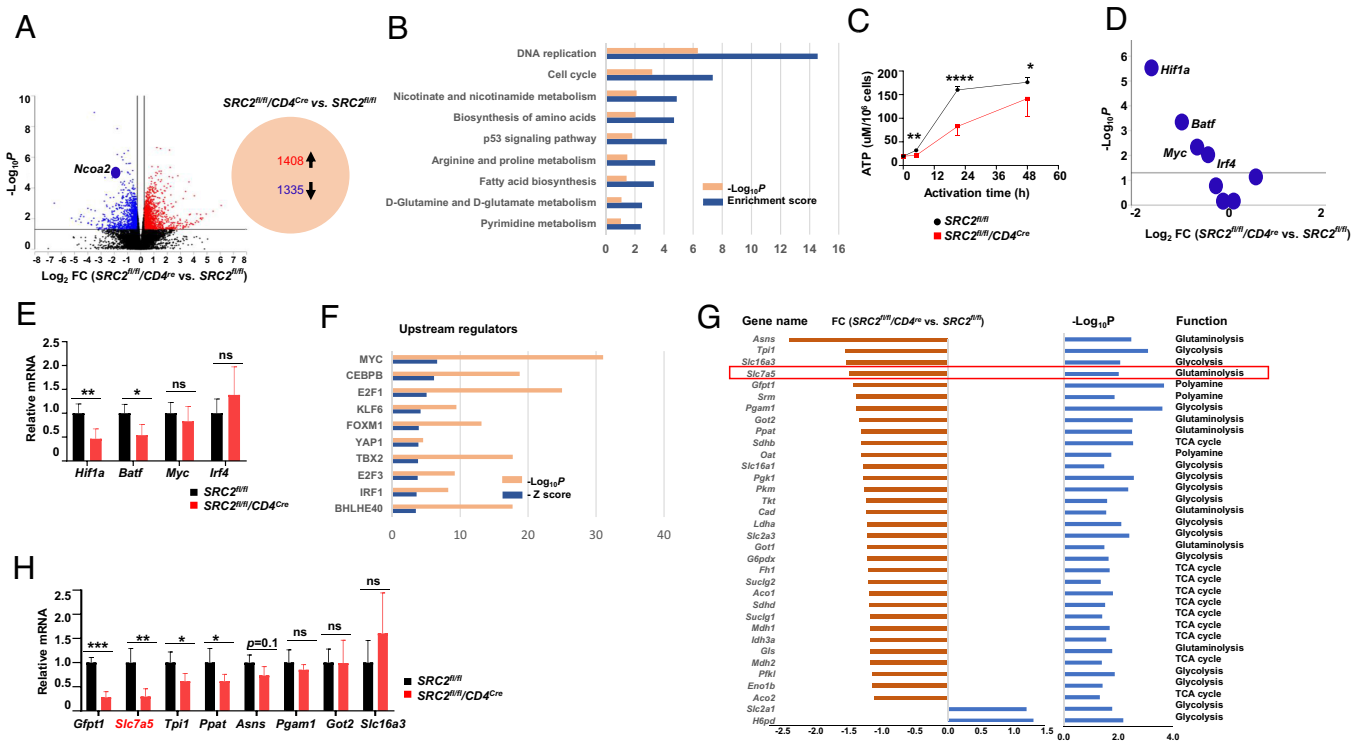

Fig. 5. CD4$^+$ T cells from *SRC2$^{fl/fl}$/CD4^{Cre}* mice are defective in c-Myc-dependent pathways. (*A*) Volcano plot comparison of gene expression between indicated CD4$^+$ cells adoptively transferred to *Rag1$^{-/-}$* recipients (n = 4 per genotype). Differentially up-regulated genes (red) and down-regulated genes (blue) with a cutoff at $P < 0.05$ and FC > 1.2. are shown. (*B*) List of the top down-regulated pathways ($P < 0.1$) in *SRC2$^{fl/fl}$/CD4^{Cre}*cells compared to WT *SRC2$^{fl/fl}$* CD4$^+$ cells. (*C*) Intracellular ATP production by indicated CD4$^+$ cells after stimulation by anti-CD3/28 antibodies for indicated times (n ≥ 6 per genotype). (*D*) Volcano plot comparison of the gene expression of top T cell metabolism regulators between *SRC2$^{fl/fl}$/CD4^{Cre}* and *SRC2$^{fl/fl}$* CD4$^+$ cells. (*E*) qPCR analysis of indicated genes in indicated CD4$^+$ cells 4 wk after being adoptively transferred to *Rag1* recipients (n ≥ 4 per genotype). (*F*) A list of predicted upstream transcription factors responsible for the changed gene expression patterns in *SRC2$^{fl/fl}$/CD4^{Cre}*CD4$^+$ T cells by IPA analysis. (*G*) A list of c-Myc-regulated metabolic genes and their function that were down-regulated in *SRC2$^{fl/fl}$/CD4^{Cre}*CD4$^+$ T cells. (*H*) qPCR analysis of indicated genes in indicated CD4$^+$ cells 4 wk after being adoptively transferred to *Rag1* recipients (n ≥ 4 per genotype). Data are from three experiments (*C*, *E* and *H*; presented as mean ± SD). *$P < 0.01$; **$P < 0.005$; ***$P < 0.001$; ****$P < 0.0005$; ns, not significant (two-tailed Students' *t* test).

impairs T cell activation-induced proliferation and cytokine production similar to the deletion of *c-Myc* or *SRC2* gene (3–6, 31). Indeed, we found a significantly down-regulated gene encoding amino acid transporter *Slc7a5* in *SRC2$^{fl/fl}$/CD4^{Cre}* CD4$^+$ cells (Fig. 5*G*), which was one of the top down-regulated genes among metabolic gene set confirmed by qPCR analysis (Fig. 5*H*). Interestingly, only *Slc7a5* was significantly down-regulated among the amino acid transporters that were reported to be regulated by c-Myc (*SI Appendix*, Fig. S7*E*) (3), indicating the selective regulation of *Slc7a5* by SRC2. Slc7a5 transports amino acids including leucine, tryptophan, and methionine, the first amino acid for all proteins, and thus is important for protein synthesis. Since Slc7a5 forms a heterodimer with CD98 and CD98 expression is greatly reduced without Slc7a5 (5), CD98 is often used as a surrogate for Slc7a5 expression (28, 32, 33). Same as the Slc7a5 expression pattern, CD98 was greatly up-regulated in activated T cells compared to naive T cells (Fig. 7*A*). However, activated *SRC2$^{fl/fl}$/CD4^{Cre}* CD4$^+$ cells failed to up-regulate CD98 to the levels detected on *SRC2$^{fl/fl}$* cells and such defective upregulation of CD98 became more dramatic when *SRC2$^{fl/fl}$/CD4^{Cre}* CD4$^+$ cells were stimulated in a nutrition-restricted medium (*SI Appendix*, Fig. S7*F*). Similarly, dramatic defective upregulation of CD98 was also found in *OT-II/SRC2$^{fl/fl}$/CD4^{Cre}* CD4$^+$ cells stimulated by different concentrations of Ova-loaded APCs (*SI Appendix*, Fig. S7*G*). Naive CD4$^+$ T cells from *OT-II* and *OT-II/SRC2$^{fl/fl}$/CD4^{Cre}* mice were transferred to *Rag1* mice that were then immunized with Ova to monitor CD98 expression in vivo (*SI Appendix*, Fig. S7*H*). CD98 expression was consistently lower in activated *OT-II/SRC2$^{fl/fl}$/CD4^{Cre}* compared to *OT-II* WT CD4$^+$ T cells (Fig. 7*B*). Next, *c-Myc* or *SRC2* gene was deleted using CRISPR/Cas9 in CD4$^+$ T cells obtained from mice expressing Cas9 and resulted in reduced T cell proliferation (*SI Appendix*, Fig. S7*I*) and downregulation of CD98 (Fig. 7*C*). Therefore, CD98 and Slc7a5 have the same expression pattern, which is regulated by c-Myc and SRC2. Consistent with the reduced expression of amino acid transporter *Slc7a5*, the capacity of amino acid uptake was significantly lower in *SRC2$^{fl/fl}$/CD4^{Cre}* CD4$^+$ T cells than that in *SRC2$^{fl/fl}$* CD4$^+$ T cells (Fig. 7*D*). Since increased uptake of amino acids stimulates mTOR pathway (5), we monitored the levels of pS6 (phosphorylated ribosomal protein S6), an indicator for mTOR activation. Indeed, pS6 levels were lower in *SRC2$^{fl/fl}$/CD4^{Cre}* CD4$^+$ cells compared to WT control (*SI Appendix*, Fig. S7*J*), consistent with the reduced amino acid uptake activity in *SRC2$^{fl/fl}$/CD4^{Cre}* CD4$^+$ cells.

To determine whether the downregulation of *Slc7a5* is responsible for the defective T cell activation in the absence of SRC2, we transduced *SRC2$^{fl/fl}$/CD4^{Cre}* CD4$^+$ T cells with the retrovirus expressing *Slc7a5*. Overexpression of *Slc7a5* greatly up-regulated CD98 in both *SRC2$^{fl/fl}$* (*SI Appendix*, Fig. S7*K*) and *SRC2$^{fl/fl}$/CD4^{Cre}* CD4$^+$ T cells (*SI Appendix*, Fig. S7*L*), confirming the positive correlation between Slc7a5 and CD98 expression. Further, forced expression of *Slc7a5* promoted proliferation (Fig. 7*E*) and Th17 differentiation (Fig. 7*F*) of *SRC2$^{fl/fl}$/CD4^{Cre}* but not obviously in *SRC2$^{fl/fl}$* CD4$^+$ T cells (*SI Appendix*, Fig. S7*M* for proliferation and S7N for Th17 differentiation) compared to the cells transduced with empty virus (EV), supporting the critical function of SRC2-regulated *Slc7a5* in T cell activation and Th17

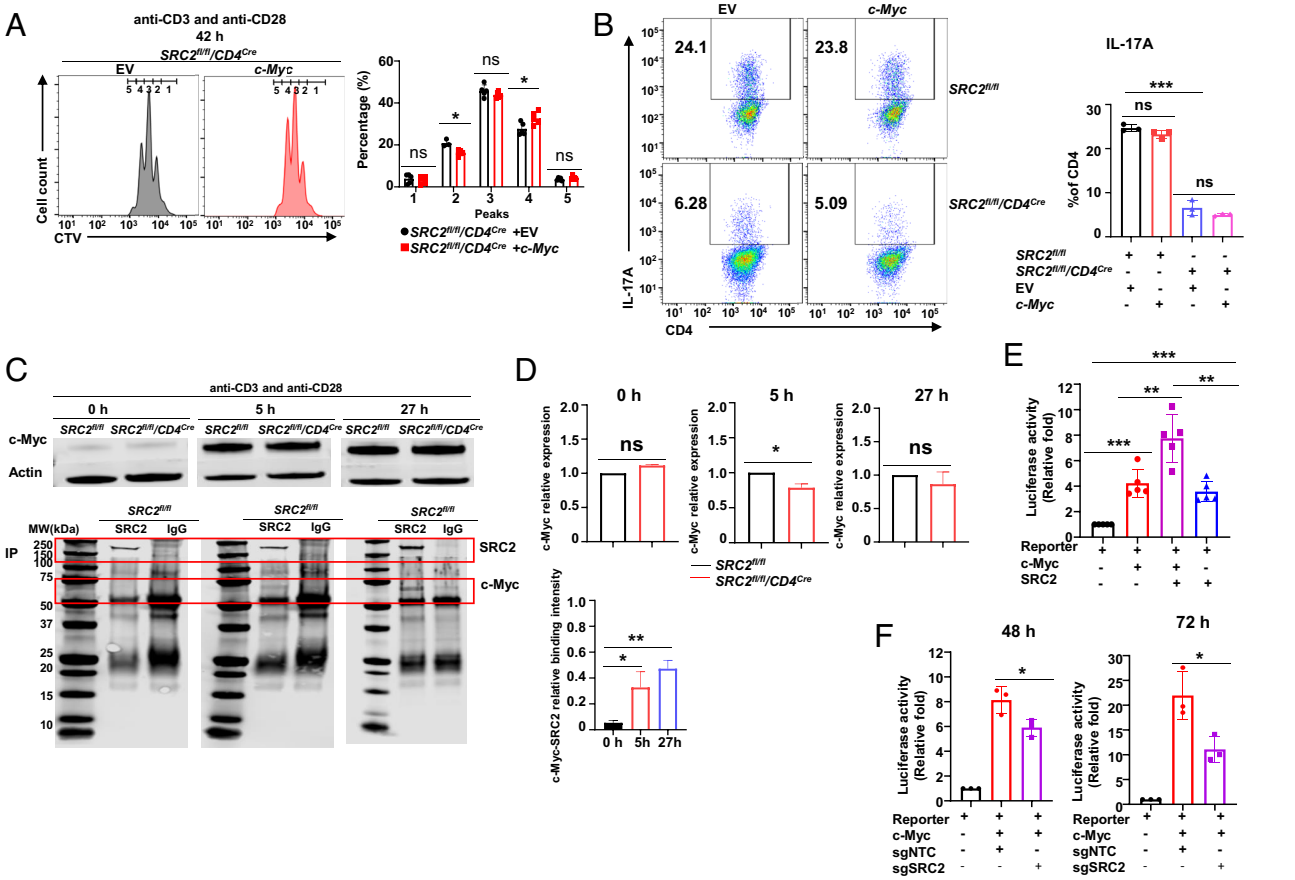

Fig. 6. c-Myc recruits SRC2 to stimulate transcription. (*A*) Representative flow cytometric analysis (*Left*) and percentage (*Right*) of the indicated proliferating CD4$^+$ T cells transduced with virus expressing Green Fluorescent Protein (GFP) alone (empty vectors, EV) or together with c-Myc, labeled with CTV, and stimulated with anti-CD3/28 antibodies for 42 h (n = 4 per genotype). (*B*) Representative flow cytometric analysis (*Left*) and the percentage (*Right*) of IL-17A$^+$ among indicated CD4$^+$ T cells transduced with retrovirus shown in *A* and differentiated under Th17 polarization conditions (n = 3 per genotype). (*C*) Immunoblot analysis of c-Myc in indicated CD4$^+$ T cells stimulated by anti-CD3/28 antibodies for indicated times (*Top*). *Bottom* panels are the immunoblot analysis of c-Myc among anti-SRC2 antibody or IgG control antibody immunoprecipitated (IP) SRC2 complexes from CD4$^+$ cells stimulated with anti-CD3/28 antibodies for indicated times. (*D*) Intensity of c-Myc band relative to the control actin shown in *Top* panels of *C* (*Top*) (n = 3 per genotype). *Bottom* panel is the intensity of c-Myc band relative to SRC2 shown in *C* (*Bottom*). (*E*) Luciferase activity from c-Myc reporter in HEK 293T cells transfected with c-Myc luciferase reporter with and without the expression plasmid for c-Myc and SRC2 for 42 h. (n = 4 per treatment). (*F*) Luciferase activity from c-Myc reporter in HEK 293T cells transfected with c-Myc luciferase reporter with and without the expression plasmid for c-Myc, nontargeting control single guide RNA (sgNTC), and single-guide RNA for deleting SRC2 (sgSRC2) for 48 h (*Left*) and 72 h (*Right*) (n= 3 per treatment). Boxed area: cell population of interest. Data are from three experiments (*D–F*; *A* and *B*, *Right* panels; presented as mean ± SD) or are from one representative of three independent experiments (*C*; *A* and *B*, *Left* panels). *P < 0.01; **P < 0.005; ***P < 0.001; ns, not significant (two-tailed Students' *t* test).

differentiation. As a control, forced expression of *Slc7a5* did not affect Th1 differentiation in either *SRC2$^{fl/fl}$* (*SI Appendix*, Fig. S7*O*) or *SRC2$^{fl/fl}$/CD4^{Cre}* (*SI Appendix*, Fig. S7*P*) cells.

Lastly, an indirect EAE model was used to determine the function of SRC2 in the regulation of *Slc7a5* in vivo. CD4$^+$ T cells from MOG$_{35-55}$-immunized *SRC2$^{fl/fl}$* and *SRC2$^{fl/fl}$/CD4^{Cre}* mice were transduced with retrovirus expressing *Slc7a5* and expanded in vitro, followed by adoptive transfer to *Rag1$^{-/-}$* for induction of EAE (Fig. 7*G*). Whereas expression of *Slc7a5* did not further enhance EAE induced by *SRC2$^{fl/fl}$* CD4$^+$ T cells, forced expression of *Slc7a5* partially restored the ability of *SRC2$^{fl/fl}$/CD4^{Cre}* CD4$^+$ T cells in the induction of EAE both in terms of severity (Fig. 7*H*) and incidence (Fig. 7*I*) of EAE. Forced expression of *Slc7a5* increased CD98 levels on *SRC2$^{fl/fl}$/CD4^{Cre}* CD4$^+$ T cells recovered from the CNS of *Rag1* mice compared to that transduced with empty virus (EV) (*SI Appendix*, Fig. S7*Q*), confirming stimulation of CD98 by *Slc7a5* expression. Consistently, the number of total CD4$^+$ T cells and pathogenic IL-17- and IFNγ-producing CD4$^+$ T cells recovered from the CNS were significantly increased by expression of *Slc7a5* in *SRC2$^{fl/fl}$/CD4^{Cre}* CD4$^+$ T cells (Fig. 7*J*), reflecting enhanced inflammation responsible for EAE by forced expression of *Slc7a5*. Altogether, our data demonstrate that SRC2, as a coactivator for c-Myc, promotes CD4$^+$ T cell-mediated immune responses by stimulating T cell activation via upregulation of amino acid transporter *Slc7a5*.

Discussion

T cell activation is critical to fully mount adaptive immune responses essential for pathogen clearance and autoimmune induction. Activated T cells have a demand for substantially increased protein synthesis activity that depends on amino acids transported by the amino acid transporters. In this study, we demonstrated the role of SRC2 in promoting the expression of amino acid transporter, *Slc7a5*, during T cell activation by interacting with c-Myc. We show that mice deficient in SRC2 in T cells (*SRC2$^{fl/fl}$/CD4^{Cre}*) have greatly impaired CD4$^+$ T cell-mediated immune responses responsible for EAE and colitis. *SRC2$^{fl/fl}$/CD4^{Cre}* mice have reduced Tregs similar to *SRC2$^{fl/fl}$/Foxp3$^{YFP\text{-}Cre}$* mice, which confirms our previous results showing that SRC2 is required for the generation of Tregs (17). However, reduced Tregs cannot explain the greatly impaired CD4$^+$ T cell-dependent immunity in *SRC2$^{fl/fl}$/CD4^{Cre}* mice, which

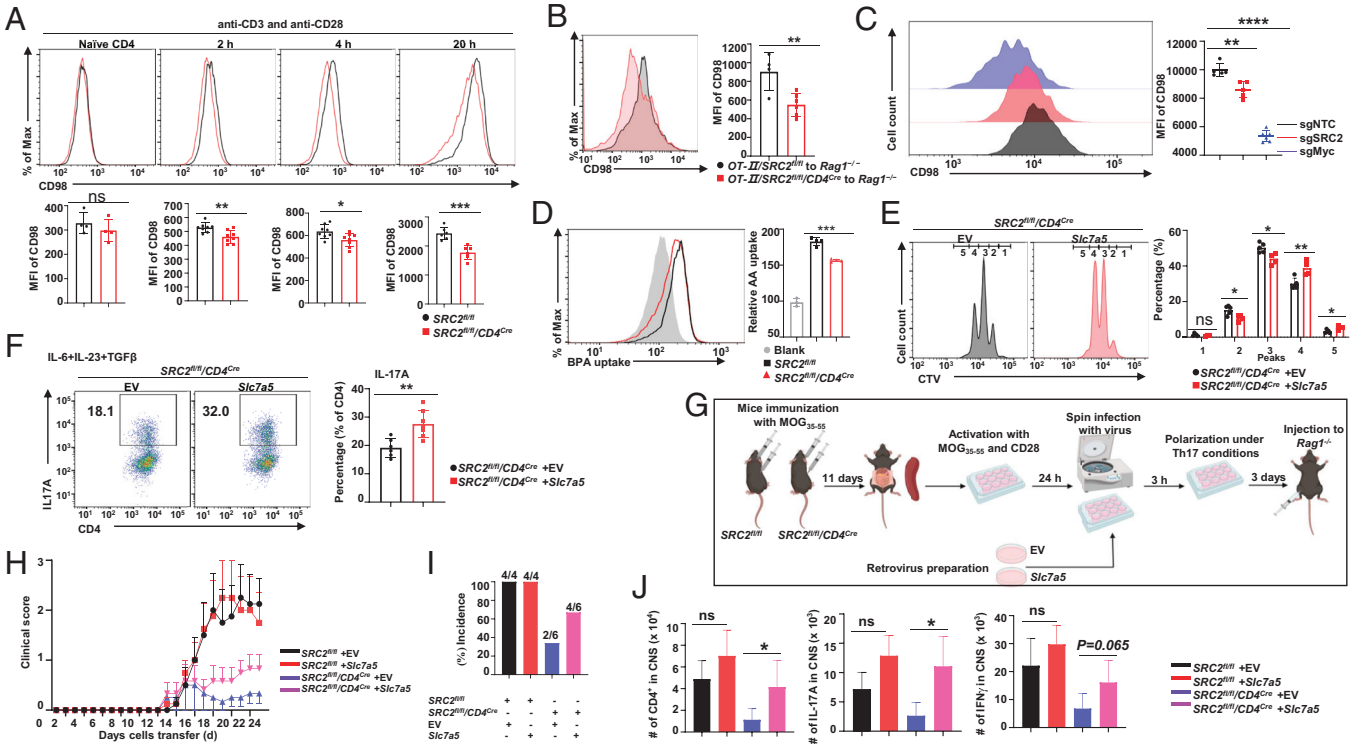

Fig. 7. SRC2 regulates CD4$^+$ T cell activation via controlling c-Myc-dependent expression of amino acid transporter *Slc7a5*. (*A*) Representative flow cytometric analysis (*Top*) and the MFI of CD98 (*Bottom*) on indicated CD4$^+$ T cells stimulated with anti-CD3/28 antibodies for indicated times (0 h, 2 h, 4 h, and 20 h) (n ≥ 4 per genotype). (*B*) Representative flow cytometric analysis (*Left*) and MFI of CD98 (*Right*) among *OT-II/SRC2$^{fl/fl}$* or *OT-II/SRC2$^{fl/fl}$/CD4^{Cre}* CD4$^+$ T cells adoptively transferred to *Rag1$^{-/-}$* recipients challenged with Ova for 1 d (n ≥ 4 per genotype). (*C*) Representative flow cytometric analysis (*Left*) and MFI of CD98 (*Right*) among CD4$^+$ T cells expressing Cas9 and transduced with retrovirus expressing sgNTC (nontargeting control), sgSRC2 (deletion of SRC2), and sgMyc (deletion of c-Myc), stimulated by anti-CD3/28 antibodies for 45 h (n = 5 per genotype). (*D*) Amino acid uptake of indicated CD4$^+$ T cells stimulated with anti-CD3/28 antibodies for 24 h (n = 4 per genotype). (*E*) Representative flow cytometric analysis (*Left*) and percentage (*Right*) of proliferating *SRC2$^{fl/fl}$/CD4^{Cre}* CD4$^+$ T cells transduced with retrovirus expressing GFP alone (empty vector, EV) or together with *Slc7a5*, labeled with CTV, and stimulated with anti-CD3/28 antibodies (n = 4 per genotype). (*F*) Representative flow cytometric analysis (*Left*) and the percentage (*Right*) of IL-17A$^+$ cells among *SRC2$^{fl/fl}$/CD4^{Cre}* CD4$^+$ T cells transduced with retrovirus expressing GFP alone (empty vector, EV) or together with *Slc7a5* and differentiated under Th17 polarization conditions (n = 5 per genotype). (*G*) Overview of the experimental procedure used for passive EAE. (*H*) Mean clinical EAE scores of *Rag1$^{-/-}$* mice different days after adoptive transfer of splenic cells obtained from MOG$_{35-55}$-primed *SRC2$^{fl/fl}$* or *SRC2$^{fl/fl}$/CD4^{Cre}* mice and transduced with retrovirus expressing GFP alone (EV) or together with *Slc7a5* (n ≥ 4 per genotype per treatment). (*I*) Incidence of paralysis of *Rag1$^{-/-}$* recipients shown in *H*. (*J*) Absolute number of CD4$^+$ (*Left*), IL-17A$^+$ cells (*Middle*), and IFNγ$^+$ cells (*Right*) in the CNS from EAE-induced *Rag1$^{-/-}$* recipients shown in *G* (n ≥ 4 per genotype per treatment). Boxed area: cell population of interest. Data are from three experiments (*H–J*; *B–F, Right* panels; *A, Bottom* panels; data in *I* and *J*; *B–F, Right* panels; *A, Bottom* panels are presented as mean ± SD; data in *H* are presented as mean ± SEM) or are from one representative of three independent experiments (*B–F, Left* panels; *A, Top* panels). *P < 0.01; **P < 0.005; ***P < 0.001; ****P < 0.0005; ns, not significant (two-tailed Students' t test).

motivates us to investigate the function of SRC2 in CD4$^+$ T cells. Our initial in vitro analysis showed impaired *SRC2$^{fl/fl}$/CD4^{Cre}* CD4$^+$ T cell proliferation, cytokine production, and Th17 differentiation in response to TCR stimulation, indicating defective T cell activation. We observed more severe defects in CD4$^+$ T cell activation in vivo analysis. CD4$^+$ T cells from *OT-II/SRC2$^{fl/fl}$/CD4^{Cre}* mice could not proliferate in vivo upon antigen (Ova) stimulation. Similarly, CD4$^+$ T cells from *SRC2$^{fl/fl}$/CD4^{Cre}* mice were unable to induce EAE or colitis. We barely recovered *SRC2$^{fl/fl}$/CD4^{Cre}* CD4$^+$ T cells from CNS in case of EAE or the gut in case of colitis, suggesting that CD4$^+$ T cells deficient of SRC2 did not migrate to the target tissues where they cause damage; additionally, these *SRC2$^{fl/fl}$/CD4^{Cre}* CD4$^+$ T cells also failed to up-regulate T cell activation markers. Such dramatic defects in CD4$^+$ T cell activation were not observed in SRC1- or SRC3-deficient cells (13), suggesting that other members of SRC family coactivators, although highly conserved, cannot compensate for the function of SRC2. Our results demonstrate that SRC2 plays the most important role in CD4$^+$ T cells among all three SRC family members.

Naive T cells express minimum levels of c-Myc, whereas T cell activation greatly stimulates c-Myc expression. The proliferation of activated T cells critically depends on increased c-Myc, which amplifies gene transcription and protein synthesis (8, 34). In response to TCR stimulation, T cells lacking c-Myc fail to increase protein content above the levels of WT naive and thus cannot proliferate and differentiate (3, 28). c-Myc regulates multiple metabolic pathways to fulfill the bioenergetic and biosynthetic demands of proliferating T cells. One of the c-Myc-regulated pathways is to promote the uptake of amino acids from the environment by stimulating the expression of amino acid transporters. T cells deficient in c-Myc fail to up-regulate several amino acid transporters, including Slc7a5 and Slc1a5, which are the most abundantly expressed on the surface of activated T cells (3). The functional importance of c-Myc-dependent upregulation of amino acid transporters is demonstrated by the lack of T cell proliferation upon stimulation if *Slc7a5* or *Slc1a5* gene is deleted (3–6). In this study, we revealed a previously unknown function of SRC2 in c-Myc-mediated upregulation of *Slc7a5* during CD4$^+$ T cell activation. T cells deficient of SRC2 or knockdown of SRC2 have lower levels of *Slc7a5* and Slc7a5-dimerizing partner CD98, similar to c-Myc deficient T cells (3), suggesting the critical role of SRC2 and c-Myc in up-regulating *Slc7a5*; SRC2 and c-Myc formed complexes in activated CD4$^+$ T cells. Further, SRC2, together with c-Myc maximally stimulates c-Myc reporter activity. These results support that SRC2 functions as a coactivator for c-Myc in stimulating *Slc7a5* expression. Lastly, forced expression of *Slc7a5* in CD4$^+$ T cells deficient in SRC2 rescues CD4$^+$ T cell proliferation and IL-17A production as well as the ability of the T cells to induce EAE. Thus, SRC2 and c-Myc-mediated upregulation of *Slc7a5* is

absolutely required for $CD4^+$ T cell activation and $CD4^+$ T cell-dependent immune responses in vivo. Although c-Myc is necessary for upregulation of both Slc7a5 and Slc1a5, T cells deficient in SRC2 only fail to up-regulate *Slc7a5* but not *Slc1a5*, suggesting a selective function of SRC2 in c-Myc-regulated gene expression. While previous reports established c-Myc as a general amplifier of gene transcription (8, 34), our results indicate that c-Myc recruits different coactivators to regulate different gene expressions.

One interesting observation is that $SRC2^{fl/fl}/CD4^{Cre}$ $CD4^+$ T cells display more dramatic defective T cell activation when activated in vivo than activated by CD3/28 cross-linking in vitro. Our results support that two factors contribute to the relatively more severe phenotypes in T cell activation in vivo: 1) physiologically relevant stimulation in vivo. Activation of $SRC2^{fl/fl}/CD4^{cre}$ CD4+ T cells by Ova-loaded APCs displayed more severe defective T cell activation including reduced activation marker CD25, decreased CD98 levels, and increased Th1 differentiation. This result suggests that strong stimulation by CD3/CD28 antibodies cross-linking in vitro partially overcomes the defective T cell activation of $SRC2^{fl/fl}/CD4^{cre}$ T cells; 2) limited nutrition availability in vivo. We observed more severe defective activation of $SRC2^{fl/fl}/CD4^{cre}$ T cells including decreased proliferation, reduced activation marker CD25, and decreased CD98 levels when they were stimulated in a nutrition-restricted medium. These results confirm long-known differences between in vitro and in vivo T cell activation.

Uncontrolled activation of T cells is responsible for various autoimmune diseases such as multiple sclerosis, type 1 diabetes, and immunological bowel disease (35, 36). On the other hand, failed T cell activation leads to severe immunodeficiency and cancer growth. Therefore, current drugs such as checkpoint inhibitors or cyclosporin A either boost or inhibit T cell activation to treat cancer and prevent transplantation rejection, respectively. Our results demonstrated the essential function of SRC2 in T cell activation and the potential clinical impact of targeting SRC2 to control T cell activation. Members of the SRC family are considered oncogenes, as they play roles in tumorigenesis in different types of cancers (37, 38). Small-molecule SRC inhibitors have already been developed for the treatment of cancers (39, 40). It would be interesting to test whether SRC2 inhibitors can prevent the above T cell-mediated autoimmunity by preventing T cell activation. Thus, our study not only reveals an important mechanism for SRC2-regulated T cell activation but also identifies SRC2 as a potential therapeutic target for T cell-mediated autoimmune diseases.

In this study, we demonstrated the critical function of SRC2 in $CD4^+$ T cell-mediated immune responses via regulating amino acid transporter Slc7a5. However, the limitation of the study includes forced expression of *Slc7a5* in $SRC2^{fl/fl}/CD4^{Cre}$ $CD4^+$ T cells only partially rescued T cell activation and EAE induction, suggesting that there are other defects in addition to failed upregulation of Slc75a. For instance, we noticed a lower ATP production whereas higher or normal extracellular acidification rate (ECAR) and oxygen consumption rate (OCR) levels in $SRC2^{fl/fl}/CD4^{Cre}$ $CD4^+$ T cells, which implies that SRC2 plays a role in other ATP generation pathways including but not limited to beta oxidation, ketosis, nucleoside diphosphate kinases, and recycled from ADP. This necessitates future work to investigate other SRC2-regulated pathways in $CD4^+$ T cell-mediated immune responses.

Materials and Methods

Detailed *Materials and Methods* can be found in *SI Appendix*.

Mice. Transgenic $CD4^{Cre}$ (*TgCd4*^{cre}, 022071), $Rag1^{-/-}$ ($Rag1^{tm1Mom}$, 002216), *Cas9* ($Rosa26^{LSL\text{-}Cas9}$, 028551), and *C57BL* (*B6*, 000664) mice were purchased from the Jackson Laboratory. $SRC2^{fl/fl}$ mice were obtained from Jianming Xu Lab (Mol & Cell Biology, Baylor College of Medicine, TX). *OT-II* mice were obtained from Jianhua Yu Lab (Department of Hematology & Hematopoietic Cell Transplantation, City of Hope, CA).

Plasmids. The retroviral vector murine stem cell virus (MSCV)-IRES-GFP was a gift from W.S. Pear (University of Pennsylvania, PA). MSCV-Slc7a5-IRES-GFP and MSCV-SRC2-IRES-GFP were made by cloning cDNA encoding *Slc7a5* and *Ncoa2* into MSCV-IRES-GFP vector. PIG-Myc (Plasmid # 177650), HA-HIF1alpha P402A/P564A-pBabe-puro (Plasmid #19005), pBABE-puro (Plasmid #1764), 7×E-Box::Renilla (Plasmid #124532), retro-gRNA-eGFP (Plasmid# 116926), and lentiCRISPR v2 (Plasmid# 52961) were purchased from Addgene.

Isolation of Naive $CD4^+$ Cells and Differentiation. Naive $CD4^+$ T cells were isolated from mice spleens by negative selection using a Naive $CD4^+$ T Cell Isolation Kit (Miltenyi Biotec). Suspensions of 5×10^5 cells/mL in RPMI-1,640 medium (Corning Inc) containing 2 mM L-glutamine, 50 μM β-mercaptoethanol, 100 U/mL penicillin, 100 mg/mL streptomycin, and 10% Fetal Bovine Serum (FBS) (Corning Inc) were cultured in 24-well or 48-well plates precoated with 0.1 mg/mL rabbit anti-hamster. The medium was supplemented with 0.25 μg/mL hamster anti-CD3 and 0.5 μg/mL hamster anti-CD28 and followed by incubation with polarizing cytokines.

In Vivo Activation and Proliferation of Naive $CD4^+$ Cells. For lymphopenia-induced proliferation, a total of 4×10^5 naive $CD4^+$ cells from $SRC2^{fl/fl}$ or $SRC2^{fl/fl}/CD4^{-Cre}$ mice were intraperitoneally injected into sex-matched $Rag1^{-/-}$ mice. For antigen-specific stimulation and activation, naive $CD4^+$ cells from $OT\text{-}II/SRC2^{fl/fl}$ or $OT\text{-}II/SRC2^{fl/fl}/CD4^{Cre}$ mice were labeled with 2.5 μM CellTrace™ Violet (CTV) (C34557, Invitrogen) and a total of 3×10^6 cells were intraperitoneally injected into sex-matched $Rag1^{-/-}$ mice or a total of 2×10^4 cells were intraperitoneally injected into sex-matched C57BL WT mice. Then, 10 μg OVA peptide (Ovalbumin (323 to 339), O1641-1MG, Sigma) mixed with Alum Adjuvant (7,7161, Thermo Scientific™) at a 1:1 ratio was also intraperitoneally injected into the recipient mice.

In Vitro Activation and Proliferation of Naive $CD4^+$ Cells. First, 5×10^5 cells/mL naive $CD4^+$ cells labeled with 2.5 μM CellTrace™ Violet (CTV) (C34557, Invitrogen) were suspended in RPMI-1,640 culture medium supplemented with either 0.25 μg/mL hamster anti-CD3 and 0.5 μg/mL hamster anti-CD28 or 5 ng/mL PMA and 1 μg/mL ionomycin. Then, to monitor T cell activation in the presence of APCs, splenic cells from $OT\text{-}II/SRC2^{fl/fl}$ or $OT\text{-}II/SRC2^{fl/fl}/CD4^{Cre}$ were cultured at 1×10^6 cells/mL in RPMI-1,640 culture medium supplemented with different concentrations of OVA peptide (0.1 μg/mL, 0.5 μg/mL, and 1.0 μg/mL). To assess the activation and proliferation under nutrition-restricted conditions, naive $CD4^+$ T cells were cultured in a Base DMEM medium (102353-100, Agilent Seahorse) supplemented with 8% FBS (Corning Inc.) and 1% nonessential amino acid (NEAA) (9304-100ML, Irvine Scientific) for 3 d.

Induction and Assessment of EAE. For active EAE, mice were immunized with 200 mg MOG_{35-55} (Hooke Laboratories) in complete Freund's adjuvant by subcutaneous injection at two dorsal sites of mice, followed by two intraperitoneal injections of 80 ng pertussis toxin (PTX) at days 0 and 1. For adoptive transferred EAE, 5×10^6 $CD4^+$ cells were adoptively transferred to sex-matched $Rag1^{-/-}$ mice. Three weeks post cell transfer, EAE was induced in $Rag1^{-/-}$ recipient mice by immunizing them with MOG_{35-55} and PTX. For passive EAE, $SRC2^{fl/fl}$ or $SRC2^{fl/fl}/CD4^{Cre}$ donor mice were immunized with MOG_{35-55} subcutaneously. After 11 d, cells were isolated from the spleen and cultured with 20 μg/mL MOG_{35-55} (DS-0111, Hooke Laboratories) and 0.5 μg/mL hamster anti-CD28 for 1 d prior to retrovirus transduction. After transduction, the cells were cultured for another 3 d with 20 μg/mL MOG_{35-55} and 0.5 μg/mL hamster anti-CD28 under Th17-polarizing conditions (2 ng/mL TGF-β, 20 ng/mL IL-6, and 20 ng/mL IL-23). *Rag1* recipient mice were then transferred intraperitoneally with 2.0×10^7 MOG_{35-55}-specific Th17 cells. The severity of EAE was monitored and evaluated on a scale from 0 to 5 according to Hooke Laboratories' guidelines.

C. rodentium Infection. Mice aged 8 to 12 wk were subjected to gavage with a 2×10^9 colony-forming unit of *C. rodentium* in 200 μL Phosphate-Buffered Saline (PBS). Mice were weighed immediately following *C. rodentium* gavage and every

other day thereafter. Three weeks after *C. rodentium* infection, the colon, spleen, and iLN were removed from mice for analysis.

Adoptive Transfer Colitis. Colitis was induced in sex-matched *Rag1*$^{-/-}$ mice by intraperitoneally injecting 4 × 10^5 naive CD4$^+$ T cells purified from the spleen of SRC2$^{fl/fl}$ or SRC2$^{fl/fl}$/CD4^{Cre} mice (8 to 10 wk old). Mice were weighed immediately following T cells transfer and weekly thereafter.

Intracellular ATP Determination. Intracellular ATP production was determined by Molecular Probes' ATP Determination Kit (A22066, Invitrogen). In brief, CD4$^+$ cells stimulated by 0.25 μg/mL hamster anti-CD3 and 0.5 μg/mL hamster anti-CD28 were harvested, counted, washed with PBS, and lysed. Luciferase activity was measured by Synergy HTX multi-mode reader (BioTek).

Metabolic Assays. The Agilent Seahorse XF Glycolysis Stress Test Kit (103020-100, Agilent Technology) and XF Cell Mito Stress Test Kit (103015-100, Agilent Technology) were used to test the ECAR in glycolysis and the OCR of activated CD4$^+$ cells. Data were analyzed using Seahorse Wave software.

Luciferase Assay. A total of 2 × 10^6 HEK 293T cells were seeded to each well of a 6-well plate and transfected with the reporter vectors 7 × E-Box::Renilla (400 ng), firefly luciferase vector (200 ng), and expression vectors (2 μg) using BioT transfection reagent (Bioland Scientific, Paramount, CA).

RNA-Seq and Analysis. Naive CD4$^+$ T cells isolated from the spleen of SRC2$^{fl/fl}$ or SRC2$^{fl/fl}$/CD4^{Cre} mice were adoptively transferred to sex-matched *Rag1*$^{-/-}$ mice. Four weeks post adoptively transfer, spleen, iLN, and mLN were removed from *Rag1*$^{-/-}$ recipient mice, and CD4$^+$ cells were purified by negative selection using CD4$^+$ T Cell Isolation Kit (Miltenyi Biotec) and subjected to RNA extraction. Each group has four replicates from different mice. Quality control, library preparation, and sequencing were performed at Novogene. The analysis was performed through Partek® Flow®.

Amino Acid Uptake Assay. The amino acid uptake capacity of CD4$^+$ cells was assessed using the amino acid uptake assay kit (#UP04–12, DOJINDO Laboratories). Briefly, CD4$^+$ cells activated for 24 h were subjected for analysis. Boronophenylalanine (BPA) was used as amino acid analogs, and the BPA uptake capacity was assessed using BPA-probe. The median fluorescent intensity (MFI) of the complex of BPA with BPA-probe in the cells was assessed using a flow cytometer.

CRISPR/Cas9-Mediated Genomic DNA Deletion. Pairs of primers containing sequences of nontargeting control (mouse) sgRNAs (sgNTC), sgRNAs targeting mouse c-Myc (sgMyc), and sgRNAs targeting mouse SRC2 (sgSRC2) were designed and cloned into a retro-gRNA-eGFP vector. Naive CD4$^+$ cells were isolated from the spleen of *Cas9* mice and transduced with the retrovirus containing sgNTC, sgMyc, and sgSRC2, respectively. The sgRNA sequences are listed in *SI Appendix*, Table S1.

Statistics and Reproducibility. The results were analyzed for statistical significance with unpaired Student's *t* test. All data are presented as mean ± SD or mean ± SEM. *P* values are calculated using GraphPad Prism and presented where the statistical significance ($P < 0.05$) was found.

Data, Materials, and Software Availability. All study data are included in the article and/or *SI Appendix*. The high-throughput sequence has been deposited in Gene Expression Omnibus with accession no. GSE229633 (41).

ACKNOWLEDGMENTS. We thank W. S. Pear for sharing the plasmids of Murine Stem Cell Virus/Internal Ribosome Entry Site/Green Fluorescent Protein (MSCV-IRES-GFP). We also thank J. Xu and J. Yu for sharing the mice strain of *SRC2*$^{fl/fl}$ and *OT-II*. Besides, we appreciate the help from the following City of Hope core facilities: Animal Resource Center, Integrative Genomics Core, Pathology Solid Tumor Core, and Bioinformatics Core. We thank Dr. Sung Hee Kil for critically reviewing and editing the manuscript. Graphical figures were created using BioRender.com. This work was supported by grants from NIH R01-AI109644, R21-AI163256, institutional pilot funding, Jackie and Bruce Barrow Cancer Research Scholars' Program, and Caltech-CoH Biomedical Initiative. Research reported in this publication included work performed in the animal, genomic, and flow cytometry cores supported under NIH grant P30CA033572. The content is solely the responsibility of the authors and does not necessarily represent the official views of the NIH.

Author affiliations: [a]Department of Immunology & Theranostics, Arthur Riggs Diabetes & Metabolism Research Institute, Beckman Research Institute of the City of Hope, Duarte, CA 91010; [b]Department of Immuno-Oncology, Beckman Research Institute of the City of Hope, Duarte, CA 91010; [c]Department of Diabetes Complication and Metabolism, Arthur Rigs Diabetes & Metabolism Research Institute, Beckman Research Institute of the City of Hope, Duarte, CA 91010; [d]Department of Physiology, David Geffen School of Medicine, University of California, Los Angeles, CA 90095; [e]Division of Translational Bioinformatic, Bioinformatics Core, City of Hope, Duarte, CA 91010; and [f]Department of Gynecology and Obsterics, School of Medicine, Emory University, Atlanta, GA 30322

1. J. E. Smith-Garvin, G. A. Koretzky, M. S. Jordan, T cell activation. *Annu. Rev. Immunol.* **27**, 591–619 (2009).
2. W. Ren *et al.*, Amino-acid transporters in T-cell activation and differentiation. *Cell Death Dis.* **8**, e2757 (2017).
3. J. M. Marchingo, L. V. Sinclair, A. J. Howden, D. A. Cantrell, Quantitative analysis of how Myc controls T cell proteomes and metabolic pathways during T cell activation. *elife* **9**, 53725 (2020).
4. K. Hayashi, P. Jutabha, H. Endou, H. Sagara, N. Anzai, LAT1 is a critical transporter of essential amino acids for immune reactions in activated human T cells. *J. Immunol.* **191**, 4080–4085 (2013).
5. L. V. Sinclair *et al.*, Control of amino-acid transport by antigen receptors coordinates the metabolic reprogramming essential for T cell differentiation. *Nat. Immunol.* **14**, 500–508 (2013).
6. M. Nakaya *et al.*, Inflammatory T cell responses rely on amino acid transporter ASCT2 facilitation of glutamine uptake and mTORC1 kinase activation. *Immunity* **40**, 692–705 (2014).
7. B. B. Au-Yeung *et al.*, IL-2 modulates the TCR signaling threshold for CD8 but not CD4 T cell proliferation on a single-cell level. *J. Immunol.* **198**, 2445–2456 (2017).
8. C. Y. Lin *et al.*, Transcriptional amplification in tumor cells with elevated c-Myc. *Cell* **151**, 56–67 (2012).
9. K. Singh *et al.*, c-MYC regulates mRNA translation efficiency and start-site selection in lymphoma. *J. Exp. Med.* **216**, 1509–1524 (2019).
10. V. H. Cowling, M. D. Cole, The Myc transactivation domain promotes global phosphorylation of the RNA polymerase II carboxy-terminal domain independently of direct DNA binding. *Mol. Cell Biol.* **27**, 2059–2073 (2007).
11. M. Yue, J. Jiang, P. Gao, H. Liu, G. Qing, Oncogenic MYC activates a feedforward regulatory loop promoting essential amino acid metabolism and tumorigenesis. *Cell Rep.* **21**, 3819–3832 (2017).
12. C. A. Walsh, L. Qin, J. C. Tien, L. S. Young, J. Xu, The function of steroid receptor coactivator-1 in normal tissues and cancer. *Int. J. Biol. Sci.* **8**, 470–485 (2012).
13. S. Sen *et al.*, SRC1 promotes Th17 differentiation by overriding Foxp3 suppression to stimulate RORgammat activity in a PKC-theta-dependent manner. *Proc. Natl. Acad. Sci. U.S.A.* **115**, E458–E467 (2018).
14. Z. He *et al.*, SRC3 is a cofactor for RORgammat in Th17 differentiation but not thymocyte development. *J. Immunol.* **202**, 760–769 (2019).
15. K. Tanaka *et al.*, Regulation of pathogenic T helper 17 cell differentiation by steroid receptor coactivator-3. *Cell Rep.* **23**, 2318–2329 (2018).
16. B. C. Nikolai *et al.*, Steroid receptor coactivator 3 (SRC-3/AIB1) is enriched and functional in mouse and human tregs. *Sci. Rep.* **11**, 3441 (2021).
17. W. Zhang *et al.*, Steroid nuclear receptor coactivator 2 controls immune tolerance by promoting induced treg differentiation via up-regulating Nr4a2. *Sci. Adv.* **8**, eabn7662 (2022).
18. S. D. Miller, W. J. Karpus, Experimental autoimmune encephalomyelitis in the mouse. *Curr. Protoc. Immunol. Chapter 15*, Unit 15–Unit 11 (2007).
19. C. P. Simmons *et al.*, Central role for B lymphocytes and CD4+ T cells in immunity to infection by the attaching and effacing pathogen citrobacter rodentium. *Infect. Immun.* **71**, 5077–5086 (2003).
20. B. A. Vallance, W. Deng, L. A. Knodler, B. B. Finlay, Mice lacking T and B lymphocytes develop transient colitis and crypt hyperplasia yet suffer impaired bacterial clearance during citrobacter rodentium infection. *Infect. Immun.* **70**, 2070–2081 (2002).
21. R. Basu *et al.*, Th22 cells are an important source of IL-22 for host protection against enteropathogenic bacteria. *Immunity* **37**, 1061–1075 (2012).
22. S. Omenetti *et al.*, The intestine harbors functionally distinct homeostatic tissue-resident and inflammatory Th17 cells. *Immunity* **51**, 77–89.e76 (2019).
23. K. Eden, Adoptive transfer colitis. *Methods Mol. Biol.* **1960**, 207–214 (2019).
24. J. Dunn, M. H. Grider, "Physiology, adenosine triphosphate" in *StatPearls* (StatPearls Publishing, Treasure Island, FL, 2022).
25. J. A. Shyer, R. A. Flavell, W. Bailis, Metabolic signaling in T cells. *Cell Res.* **30**, 649–659 (2020).
26. L. Z. Shi *et al.*, HIF1alpha-dependent glycolytic pathway orchestrates a metabolic checkpoint for the differentiation of TH17 and Treg cells. *J. Exp. Med.* **208**, 1367–1376 (2011).
27. E. V. Dang *et al.*, Control of T(H)17/T(reg) balance by hypoxia-inducible factor 1. *Cell* **146**, 772–784 (2011).
28. R. Wang *et al.*, The transcription factor Myc controls metabolic reprogramming upon T lymphocyte activation. *Immunity* **35**, 871–882 (2011).
29. H. Tan *et al.*, Integrative proteomics and phosphoproteomics profiling reveals dynamic signaling networks and bioenergetics pathways underlying T cell activation. *Immunity* **46**, 488–503 (2017).
30. T. Lindsten, C. H. June, C. B. Thompson, Multiple mechanisms regulate c-myc gene expression during normal T cell activation. *EMBO J.* **7**, 2787–2794 (1988).
31. J. Cantor, M. Slepak, N. Ege, J. T. Chang, M. H. Ginsberg, Loss of T cell CD98 H chain specifically ablates T cell clonal expansion and protects from autoimmunity. *J. Immunol.* **187**, 851–860 (2011).
32. M. C. Poffenberger, R. G. Jones, Amino acids fuel T cell-mediated inflammation. *Immunity* **40**, 635–637 (2014).
33. H. Jensen, M. Potempa, D. Gotthardt, L. L. Lanier, Cutting edge: IL-2-induced expression of the amino acid transporters SLC1A5 and CD98 is a prerequisite for NKG2D-mediated activation of human NK cells. *J. Immunol.* **199**, 1967–1972 (2017).

34. Z. Nie *et al.*, c-Myc is a universal amplifier of expressed genes in lymphocytes and embryonic stem cells. *Cell* **151**, 68–79 (2012).
35. Z. Huang, H. Xie, R. Wang, Z. Sun, Retinoid-related orphan receptor gamma t is a potential therapeutic target for controlling inflammatory autoimmunity. *Expert Opin. Ther. Targets* **11**, 737–743 (2007).
36. J. Zhu, H. Yamane, W. E. Paul, Differentiation of effector CD4 T cell populations (*). *Annu. Rev. Immunol.* **28**, 445–489 (2010).
37. A. D. Rohira *et al.*, Targeting SRC coactivators blocks the tumor-initiating capacity of cancer stem-like cells. *Cancer Res.* **77**, 4293–4304 (2017).
38. S. Suresh *et al.*, SRC-2-mediated coactivation of anti-tumorigenic target genes suppresses MYC-induced liver cancer. *PLoS Genet.* **13**, e1006650 (2017).
39. X. Song *et al.*, Development of potent small-molecule inhibitors to drug the undruggable steroid receptor coactivator-3. *Proc. Natl. Acad. Sci. U.S.A.* **113**, 4970–4975 (2016).
40. Y. Wang *et al.*, Small molecule inhibition of the steroid receptor coactivators, SRC-3 and SRC-1. *Mol. Endocrinol.* **25**, 2041–2053 (2011).
41. Z. Sun, W. Zhang, SRC2 controls CD4+ T cell activation via stimulating c-Myc-mediated up-regulation of amino acid transporterSlc7a5. Gene Expression Omnibus. https://www.ncbi.nlm.nih.gov/geo/query/acc.cgi?acc=GSE229633. Deposited 12 April 2023.